

Novel Functional Graded Thermal Barrier Coatings in Coal-fired Power Plant Turbines

Jing Zhang

Department of Mechanical Engineering
Indiana University-Purdue University Indianapolis

Grant No.: DOE DE-FE0008868
Program Manager: Richard Dunst

IUPUI

**INDIANA UNIVERSITY
PURDUE UNIVERSITY
INDIANAPOLIS**

Acknowledgement



- Subcontract: James Knapp (Praxair Surface Technologies)
- Collaborators: Li Li, Don Lemen (Praxair Surface Technologies)
- Yeon-Gil Jung (Changwon National University)
- Yang Ren (Argonne National Laboratory)
- Graduate students: Xingye Guo, Yi Zhang

Outline

- **I. Introduction**
 - $\text{La}_2\text{Zr}_2\text{O}_7$ vs. YSZ
 - Multilayer TBC structure
- **II. Experiments**
 - High density $\text{La}_2\text{Zr}_2\text{O}_7$
 - Low density $\text{La}_2\text{Zr}_2\text{O}_7$
- **III. Theoretical study of properties of $\text{La}_2\text{Zr}_2\text{O}_7$**
- **IV. Summary**

Limitation of yttria stabilized zirconia

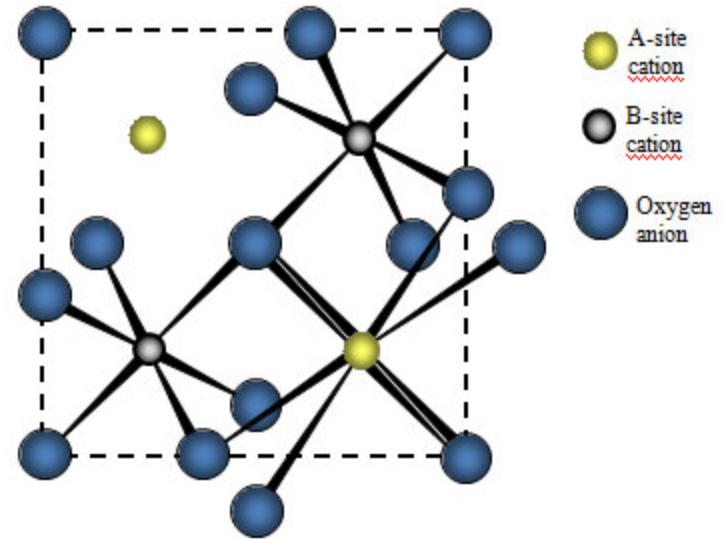
- Zirconia partially stabilized with 7 wt% yttria (7YSZ) is the current state-of-the-art thermal barrier coating material.
- However, at temperatures higher than 1200 °C, YSZ layers are prone to **sintering**, which increases thermal conductivity and makes them less effective.
- The sintered and densified coatings can also **reduce thermal stress and strain tolerance**, which can reduce the coating's durability significantly.

Motivation and objective

- To further increase the operating temperature of turbine engines, alternate TBC materials with lower thermal conductivity, higher operating temperatures and better sintering resistance are required.
- The objective of the project is to develop a novel lanthanum zirconate based multi-layer thermal barrier coating system.
- The ultimate goal is to develop a manufacturing process to produce pyrochlore oxide based coating with improved high-temperature properties.

Pyrochlore - $A_2B_2O_7$

Pyrochlore-type rare earth zirconium oxides ($Re_2Zr_2O_7$, $Re =$ rare earth) are promising candidates for thermal barrier coatings, high-permittivity dielectrics, potential solid electrolytes in high-temperature fuel cells, and immobilization hosts of actinides in nuclear waste.

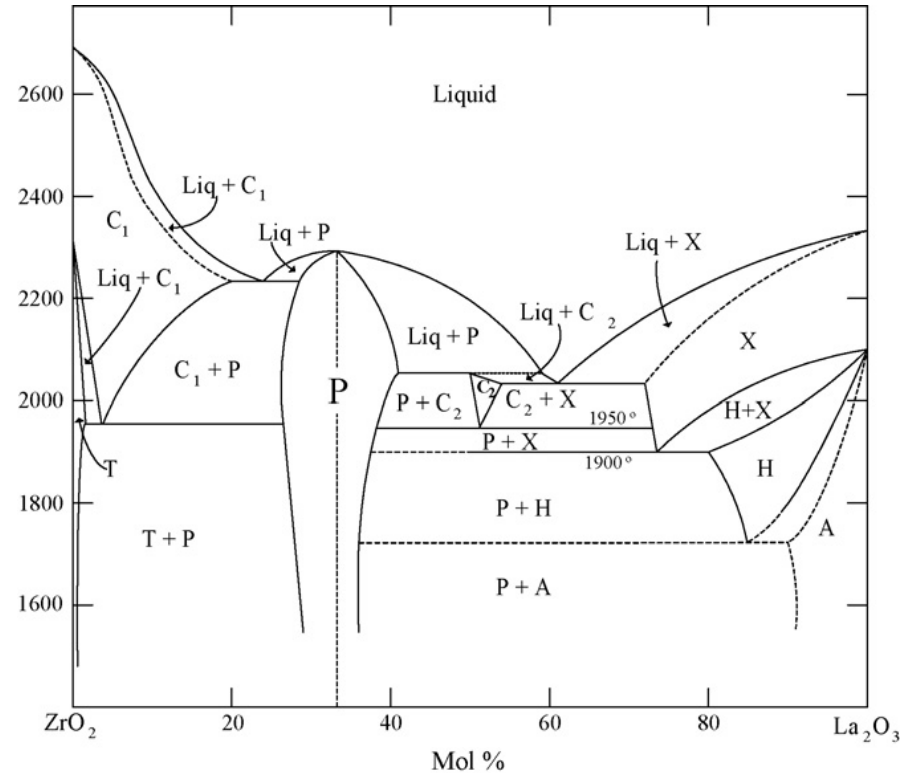


Pyrochlore crystal structure: $A_2B_2O_7$. A and B are metals incorporated into the structure in various combinations. (credit: NETL)

Why $\text{La}_2\text{Zr}_2\text{O}_7$?

Compared with YSZ, $\text{La}_2\text{Zr}_2\text{O}_7$ has

- Higher temperature phase stability. No phase transformation
- Lower sintering rate at elevated temperature
- Lower thermal conductivity
- Lower CTE (can be enhanced by CeO_2 doping)



Phase diagram of La_2O_3 - ZrO_2

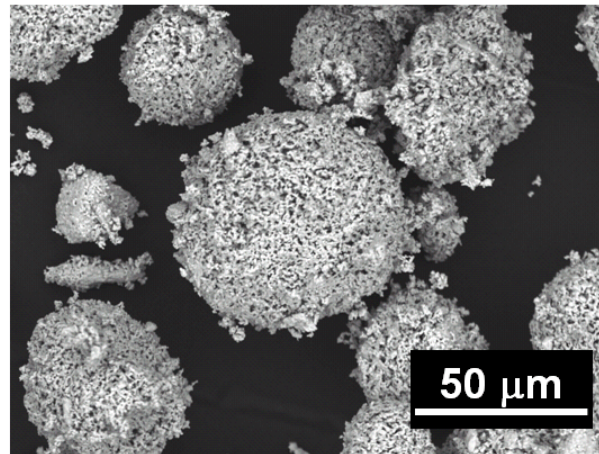
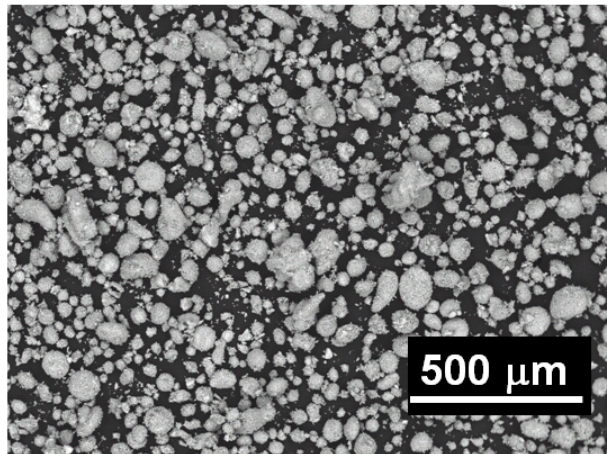
YSZ vs. $\text{La}_2\text{Zr}_2\text{O}_7$

Materials property	8YSZ	$\text{La}_2\text{Zr}_2\text{O}_7$
Melting Point ($^{\circ}\text{C}$)	2680	2300
Maximum Operating Temperature ($^{\circ}\text{C}$)	1200	>1300
Thermal Conductivity (W/m-K) (@ 800 $^{\circ}\text{C}$)	2.12	1.6
Coefficient of Thermal Expansion ($\times 10^{-6}/\text{K}$) (@1000 $^{\circ}\text{C}$)	11.0	8.9-9.1
Density (g/cm^3)	6.07	6.00
Specific heat (J/g-K) (@1000 $^{\circ}\text{C}$)	0.64	0.54

Layered coating architecture

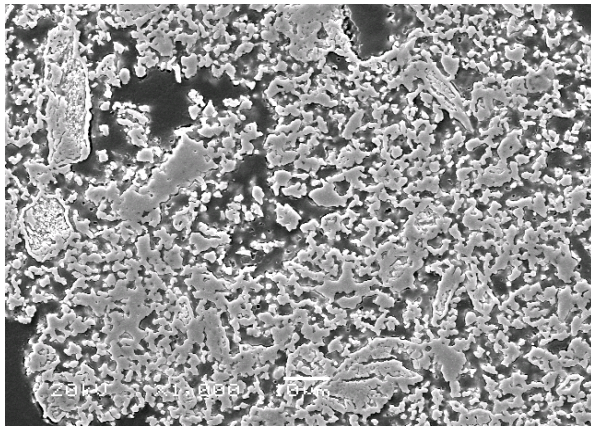
- The coefficient of thermal expansion of $\text{La}_2\text{Zr}_2\text{O}_7$ ($10 \times 10^{-6}/\text{K}$) is lower than those of both substrate and bondcoat (about $15 \times 10^{-6}/\text{C}$ @ 1000°C). As a result, the thermal cycling properties may be a concern
- The layered topcoat architecture is believed to be a feasible solution to improve thermal strain tolerance
- In this work, we develop a multi-layer, functionally graded, pyrochlore oxide based TBC system

La₂Zr₂O₇ powder morphology

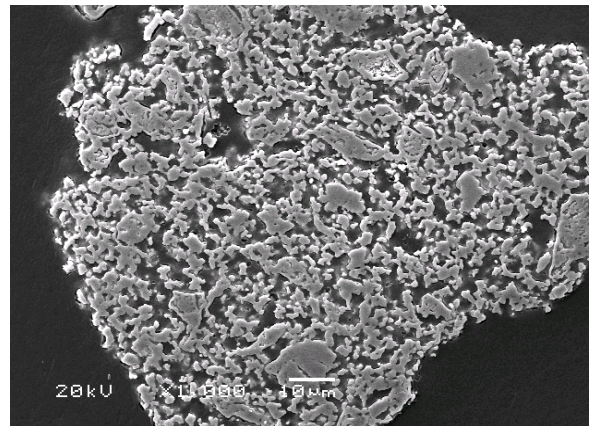


Powder surface morphology

- Spherical shape with rough surface
- Good flowability and high density
- Particle size between 30 ~ 100 μm



+ 125 μm

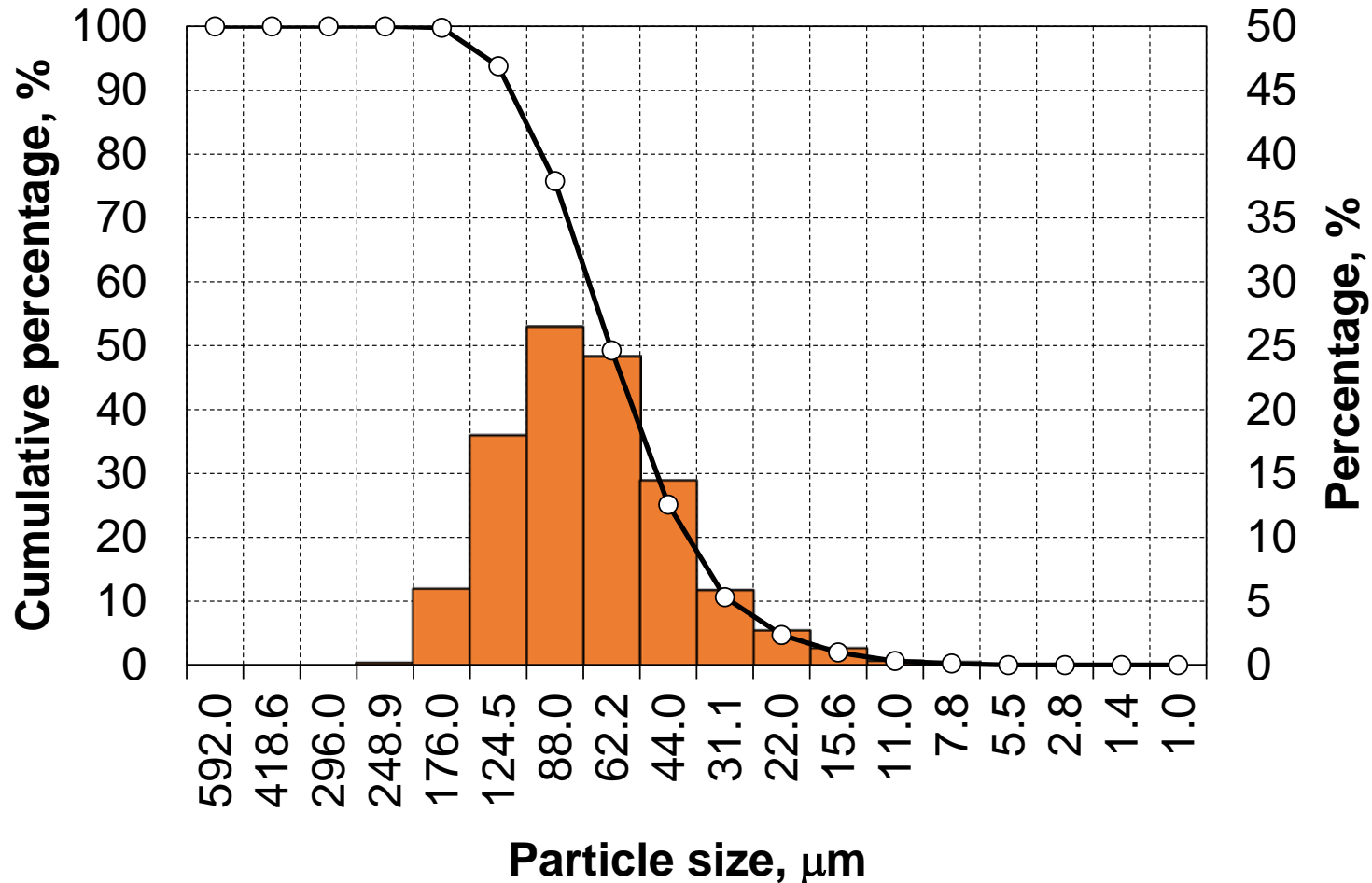


- 125 μm

Powder cross-section

- Porous interior

Powder size distribution (PSD)



Microtrac standard range particle analyzer's percent passing data show that the average powder size, D_{50} , is $\sim 65 \mu\text{m}$

Chemical composition - ICP-MS

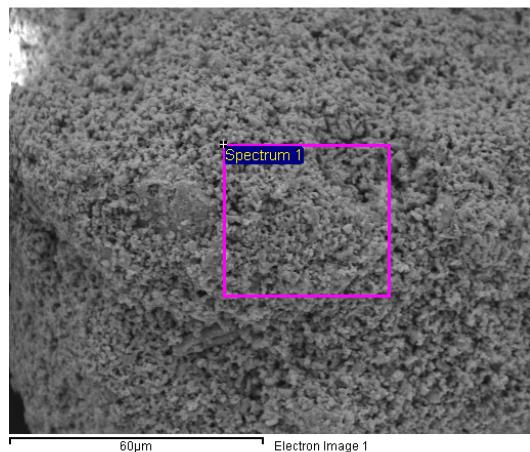
All elements measured in weight percent unless otherwise specified. Sampling Method per ASTM B215.

Chemistry	Test Method	Test Lab	Min	Max	Result	OK
Aluminum Oxide	ICP	NSL Analytical Services		0.2	<0.1	Yes
Ferric Oxide	ICP-MS	NSL Analytical Services		0.5	0.1	Yes
Hafnium Oxide	ICP	NSL Analytical Services		2.5	0.8	Yes
Lanthanum Oxide	By Difference	NSL Analytical Services			57	Yes
Other Oxides Total	ICP-MS	NSL Analytical Services		1.5	0.4	Yes
Silicon Dioxide	ICP	NSL Analytical Services		1.0	0.7	Yes
Titanium Dioxide	ICP-MS	NSL Analytical Services		0.5	0.0	Yes
Uranium + Thorium	ICP-MS	NSL Analytical Services		0.05	0.02	Yes
Zirconium Oxide	ICP	NSL Analytical Services			41	Yes

- Inductively coupled plasma – mass spectrometry (ICP-MS) technique was used to measure the powder compositions
- The measurements confirms $\text{La}_2\text{Zr}_2\text{O}_7$ composition

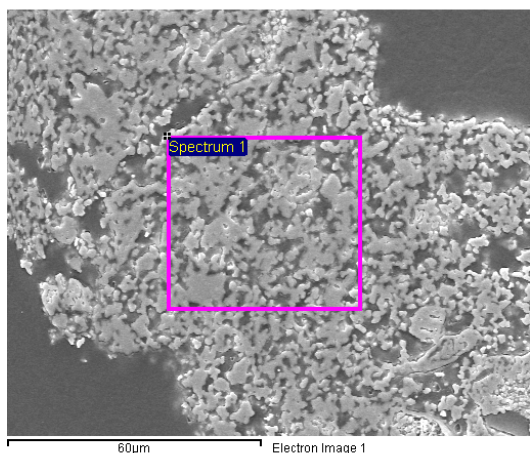
Element analysis of cross-section

Powder surface



Element	Weight%	Atomic%
O K	28.51	74.28
Zr L	27.21	12.43
La L	44.28	13.29
Total	100	

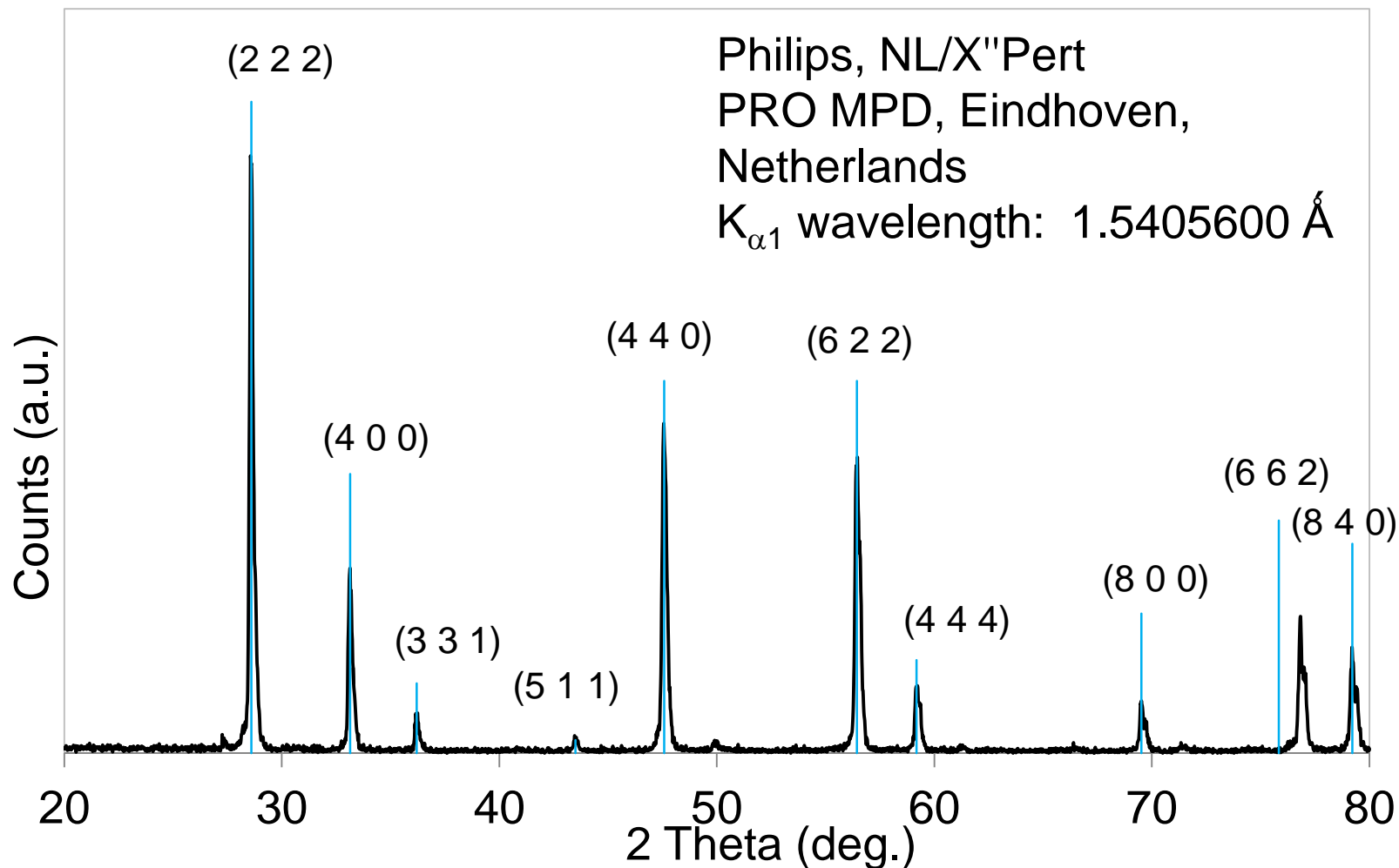
Powder cross-section



Element	Weight%	Atomic%
O K	17.42	60.37
Zr L	31.92	19.40
La L	50.67	20.23
Total	100	

Higher La, and lower Zr and O contents are inside of powder than on surface

La₂Zr₂O₇ powder XRD analysis



XRD data show that the powder composition is La₂Zr₂O₇

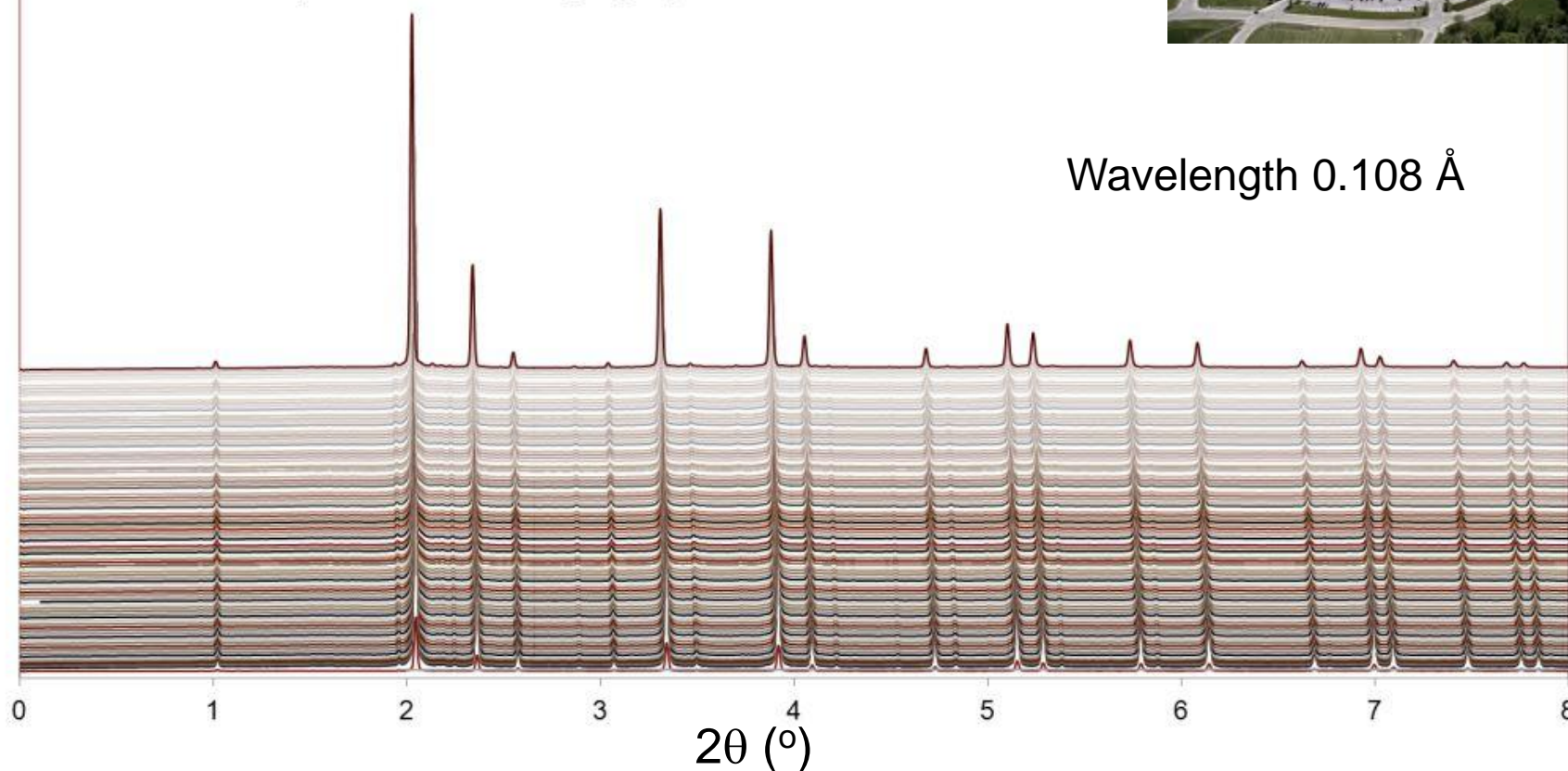
Synchrotron XRD



In situ HEXRD profiles of $\text{La}_2\text{Zr}_2\text{O}_7$ from 30°C to 1400°C

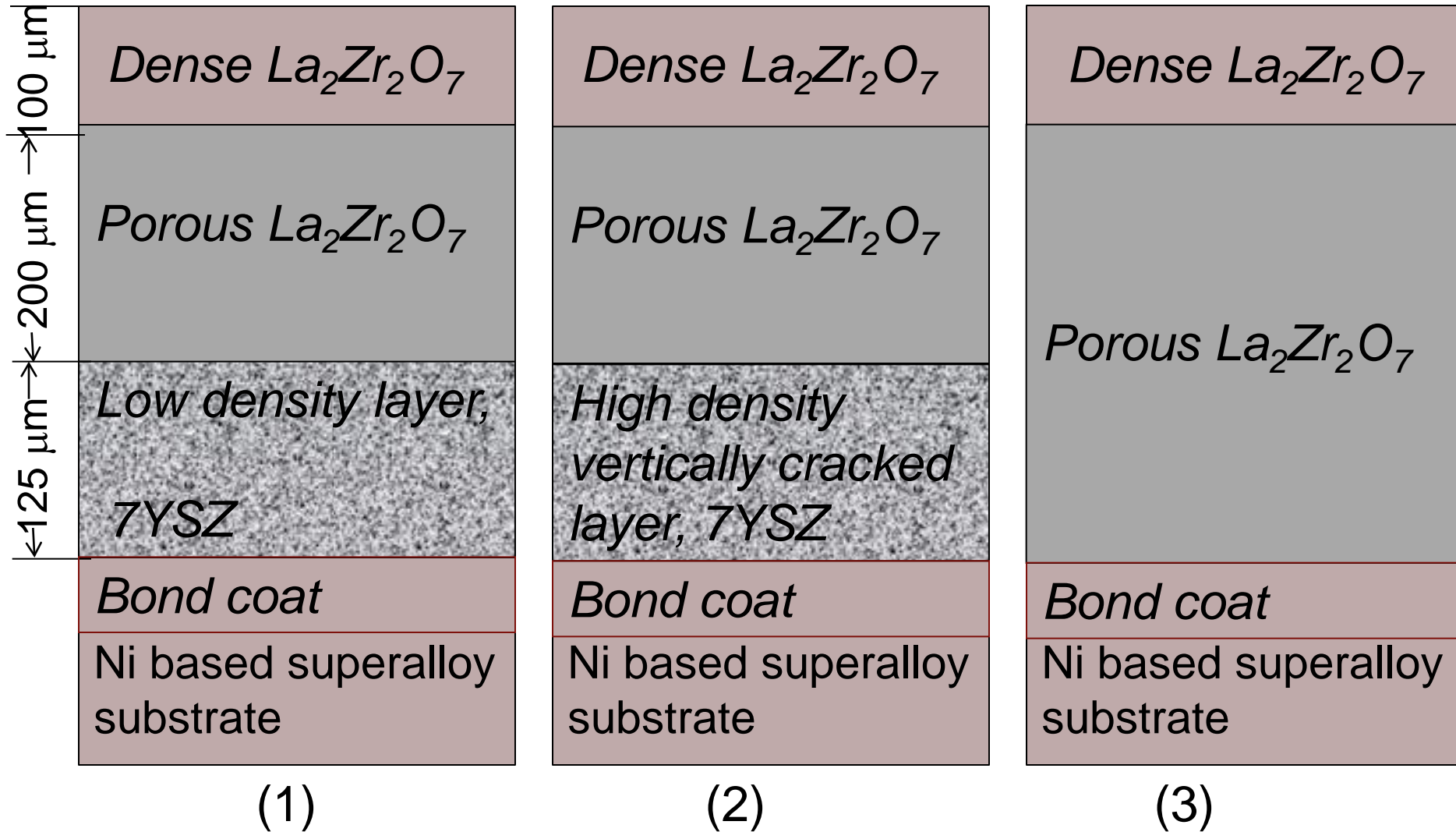
Wavelength 0.108 Å

Count (a.u.)



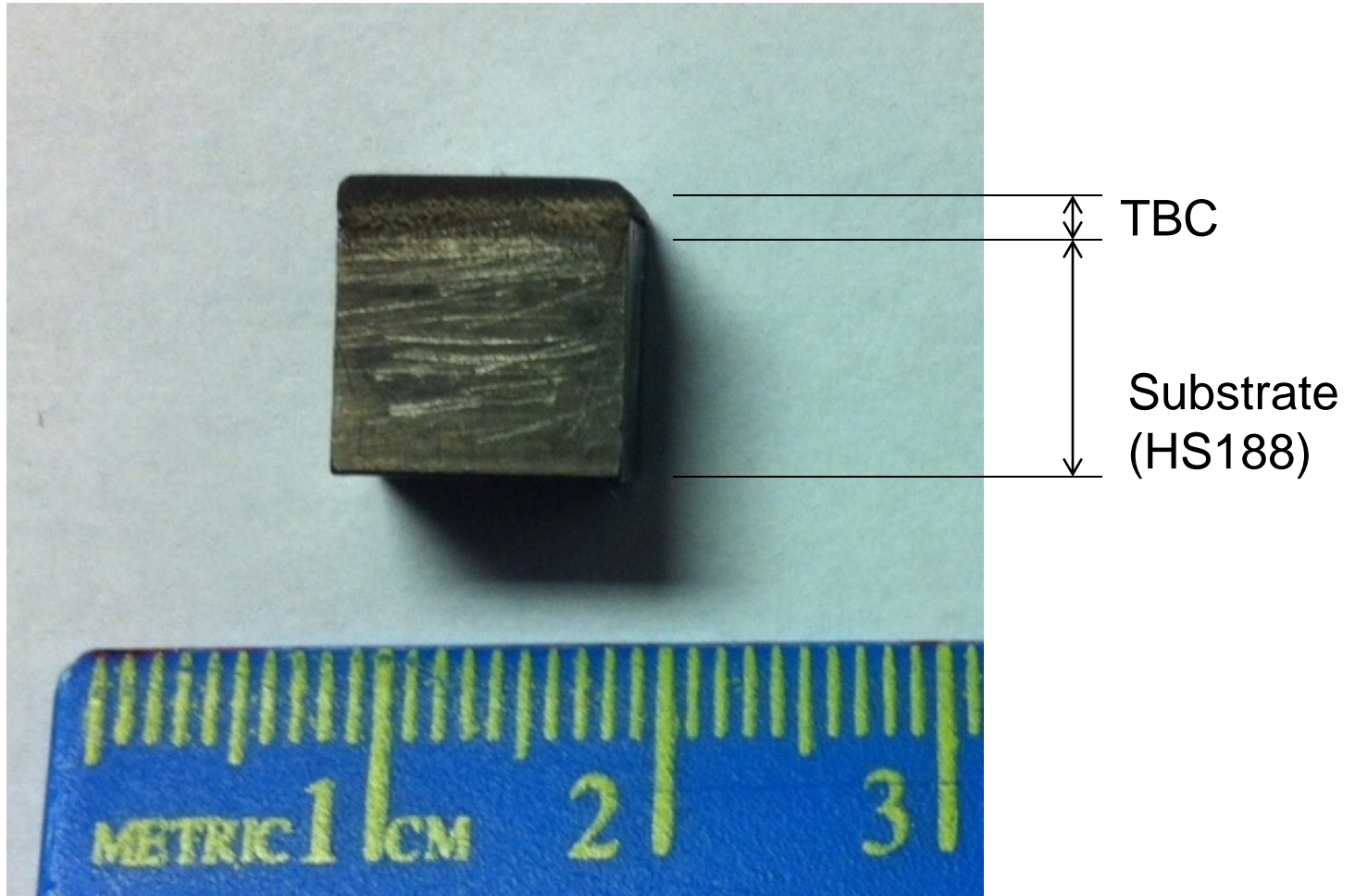
In situ Synchrotron XRD shows no compositional change at high temperatures

Design of Layered TBCs

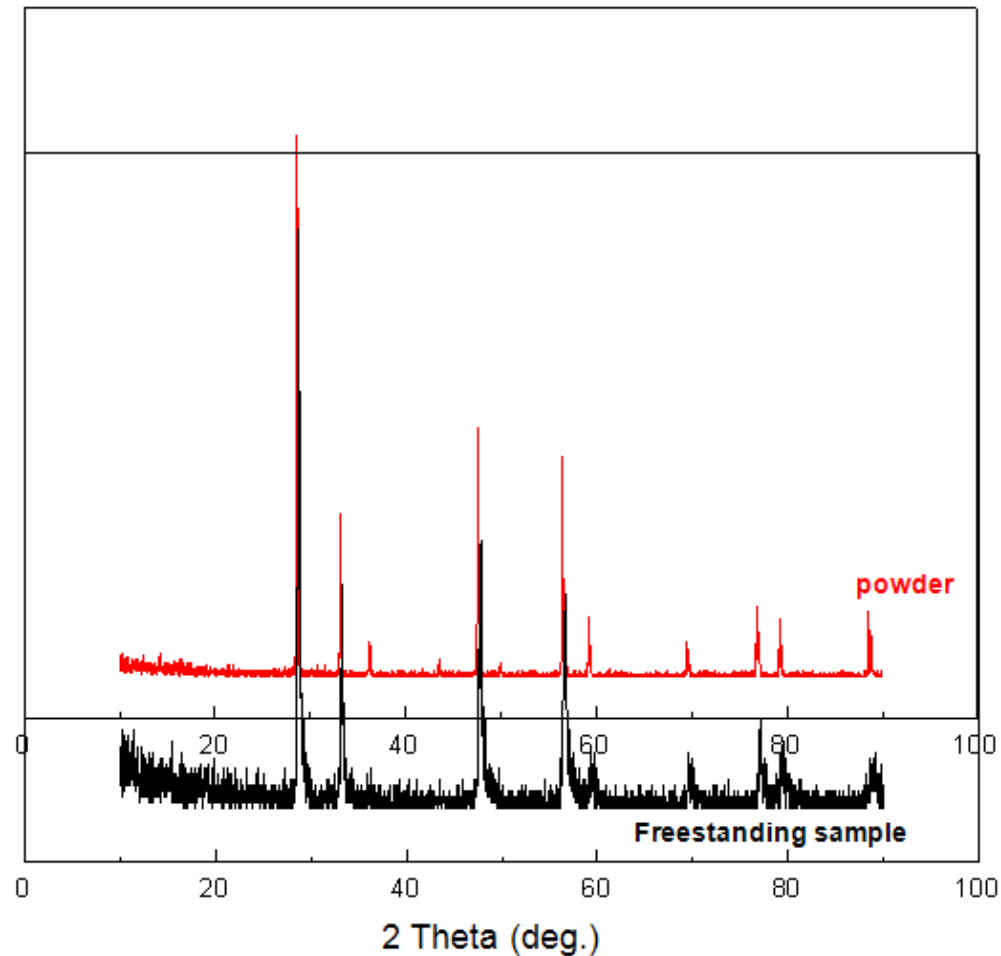


- **I. Introduction**
 - $\text{La}_2\text{Zr}_2\text{O}_7$ vs. YSZ
 - Multilayer TBC structure
- **II. Experiments**
 - High density $\text{La}_2\text{Zr}_2\text{O}_7$
 - Low density $\text{La}_2\text{Zr}_2\text{O}_7$
- **III. Theoretical study of properties of $\text{La}_2\text{Zr}_2\text{O}_7$**
- **IV. Summary**

Dense coating

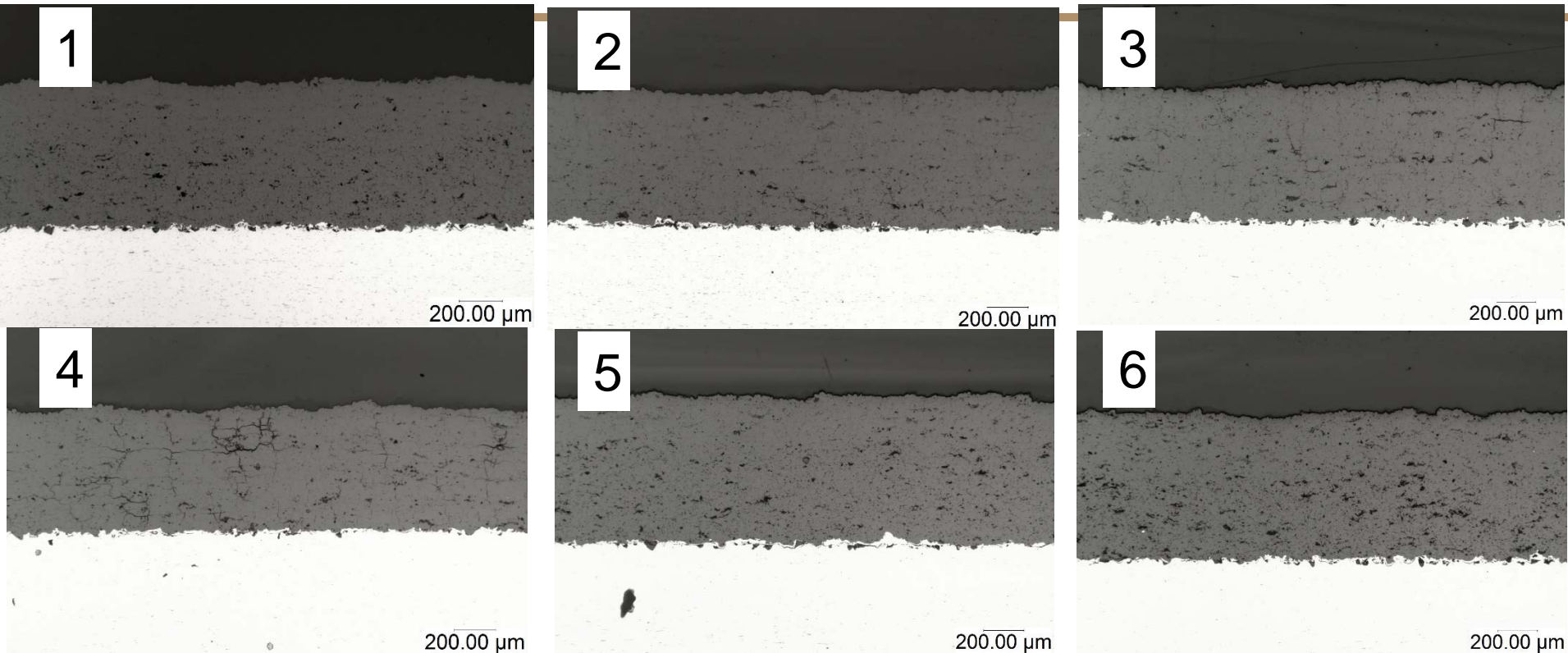


XRD analysis of coating and powder



XRD shows that coating compositions are same as those of the powder

Cross section view of dense coating

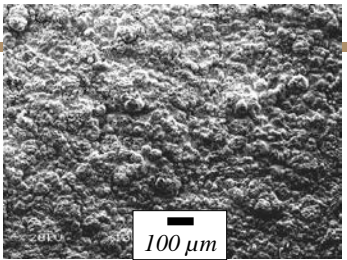
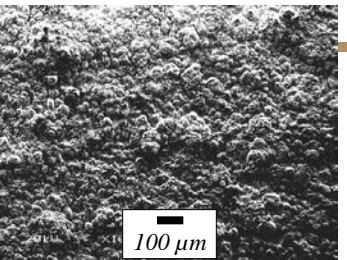
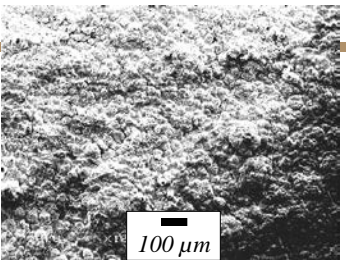


Processing parameters (powder feed rate, surface speed, current, stand off) were varied to control the porosity.

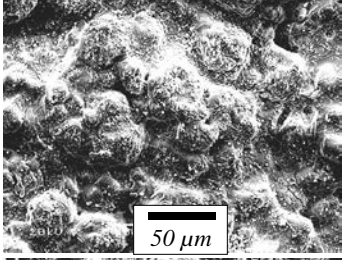
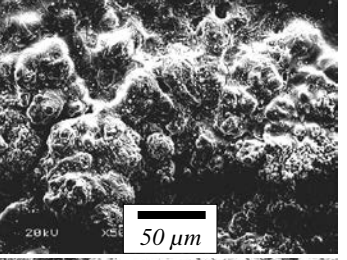
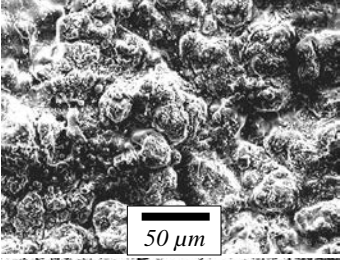
Surface microstructures

5279-14 line #2

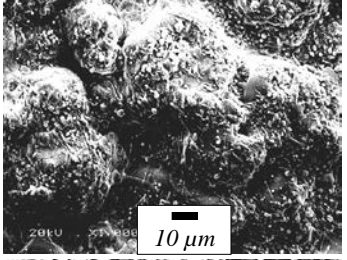
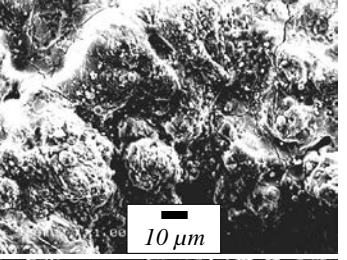
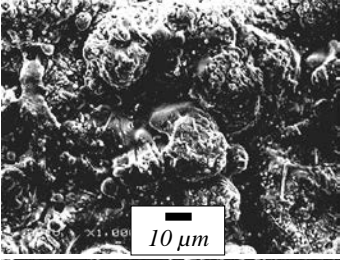
X100



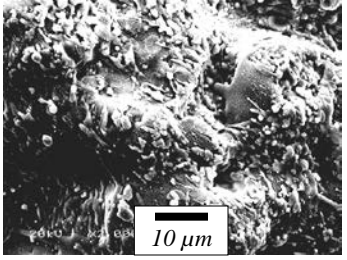
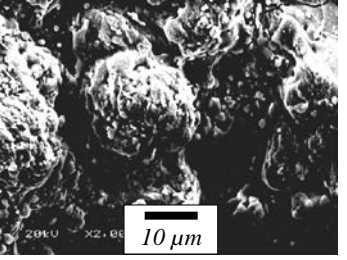
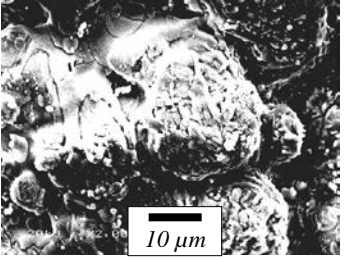
X500



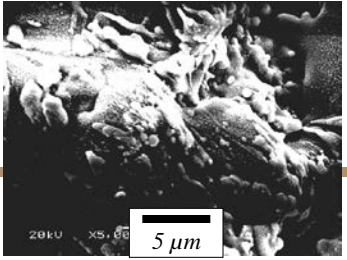
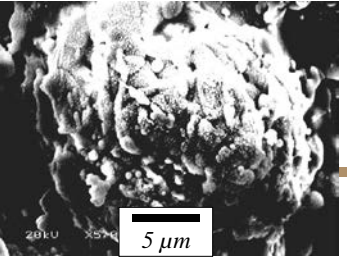
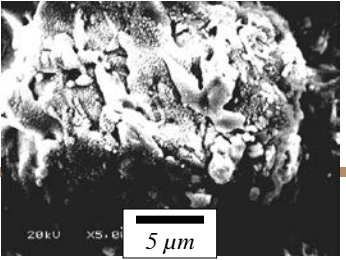
X1000



X2000

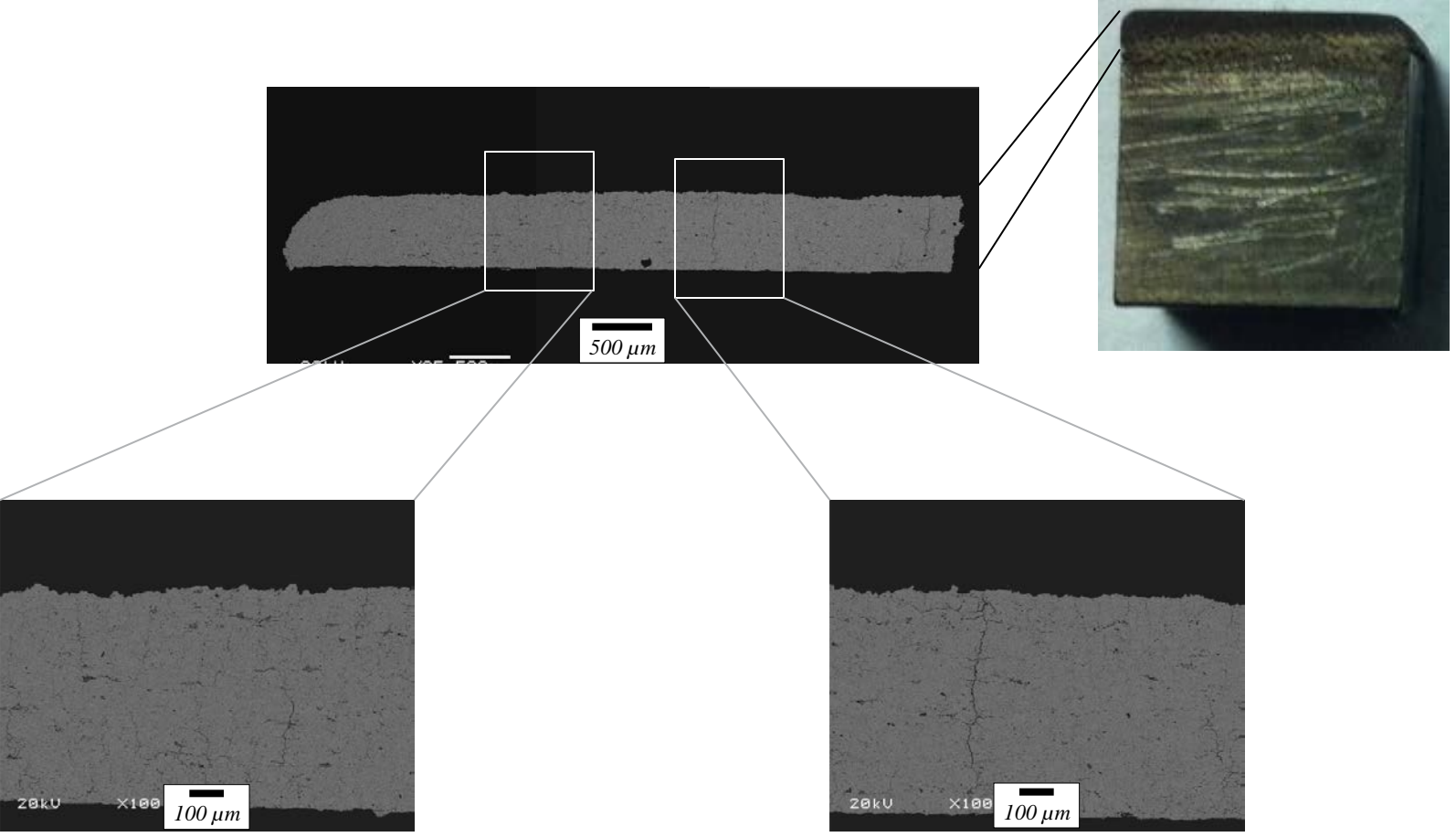


X5000



Backscattered SEM images

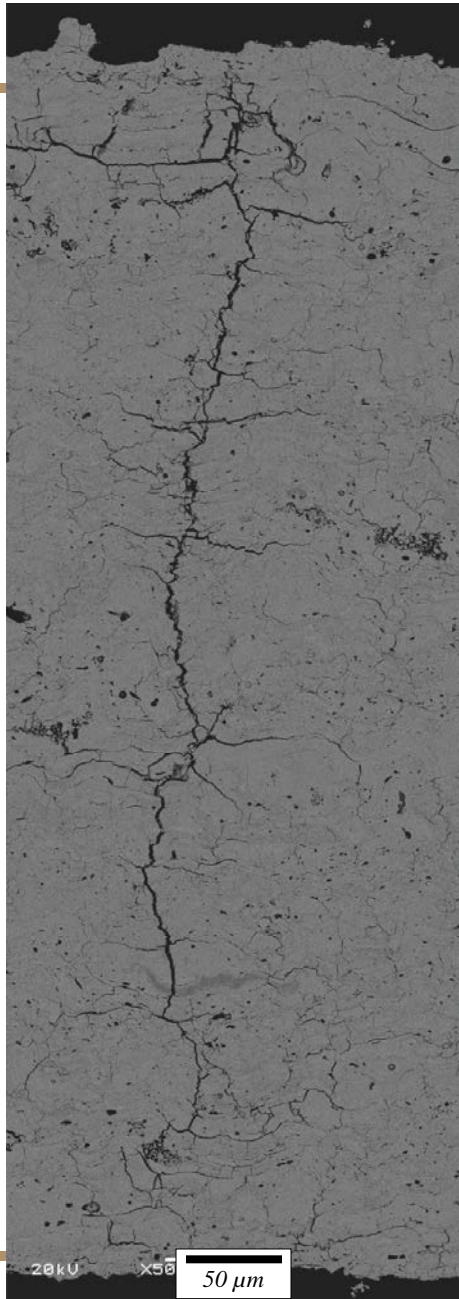
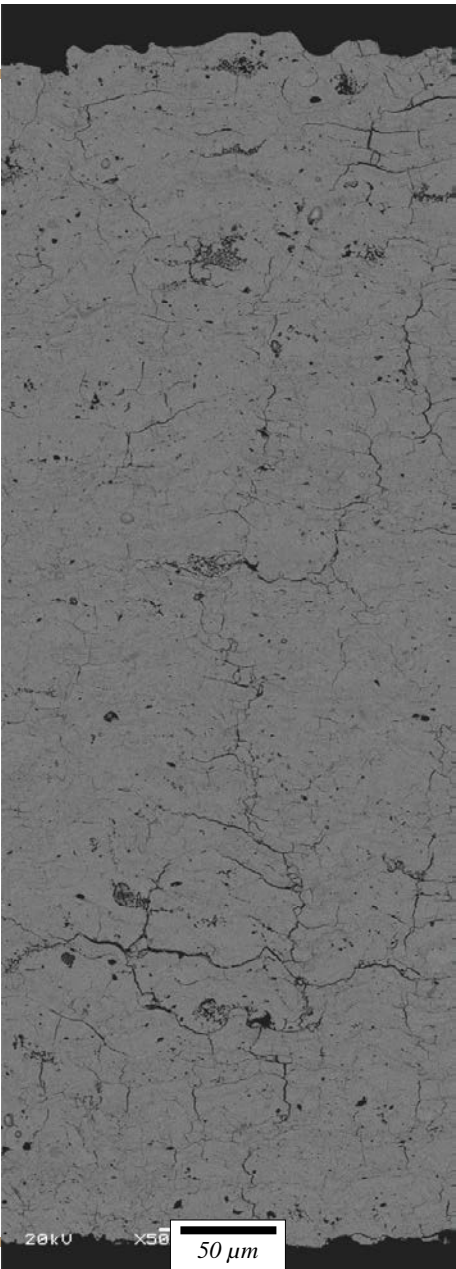
5279-14 line #2



Dense vertical crack (DVC)

Backscattered SEM images (cont'd)

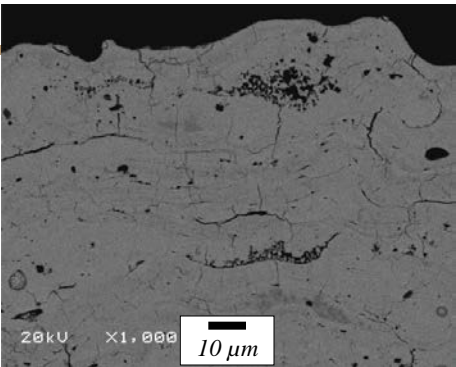
5279-14 line #2



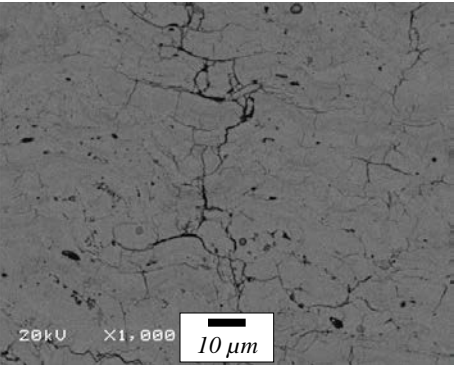
Dense vertical crack (DVC)

Backscattered SEM images (cont'd)

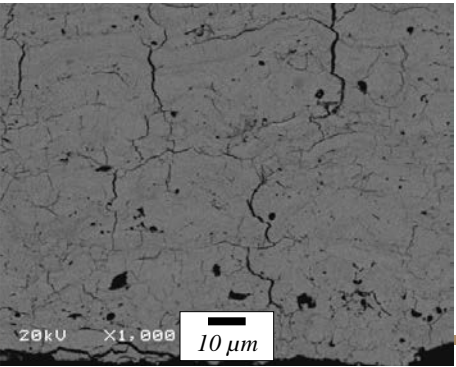
5279-14 line #2



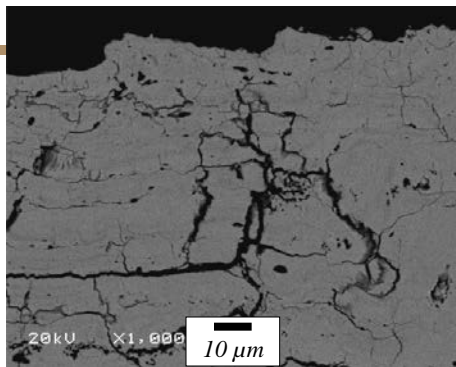
Top



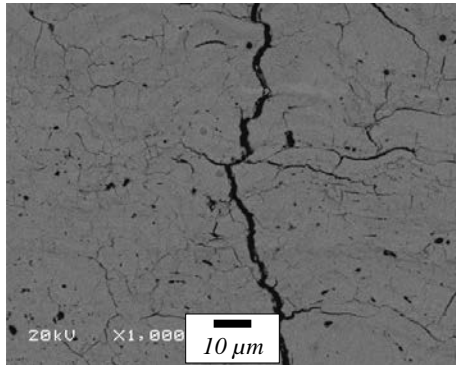
Middle



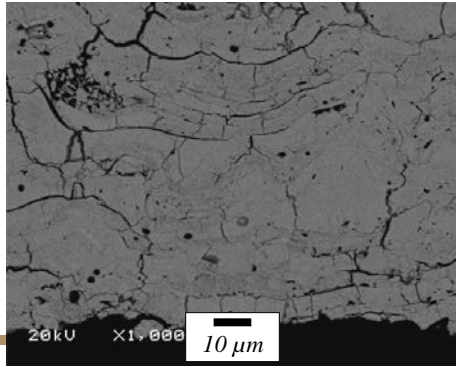
Bottom



Top

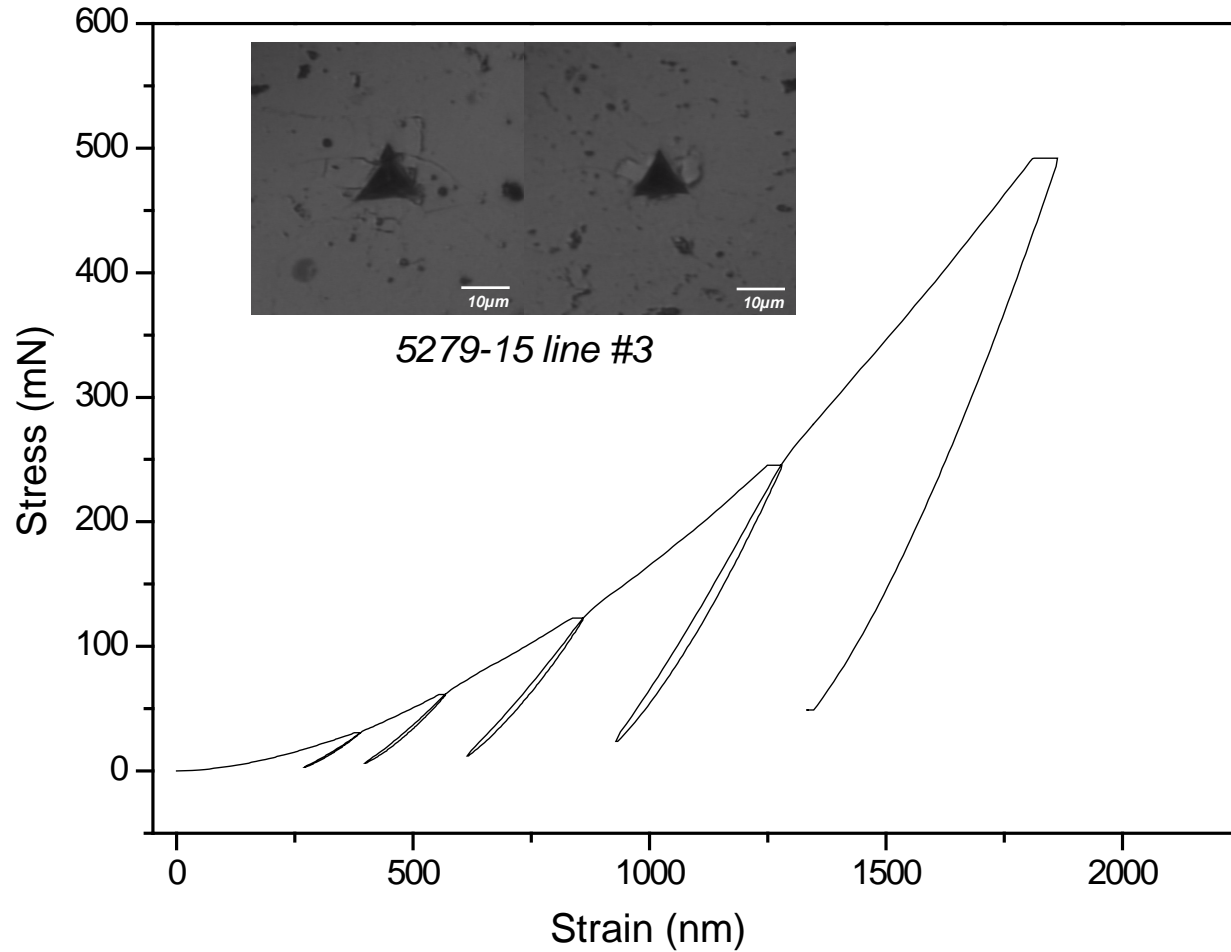


Middle

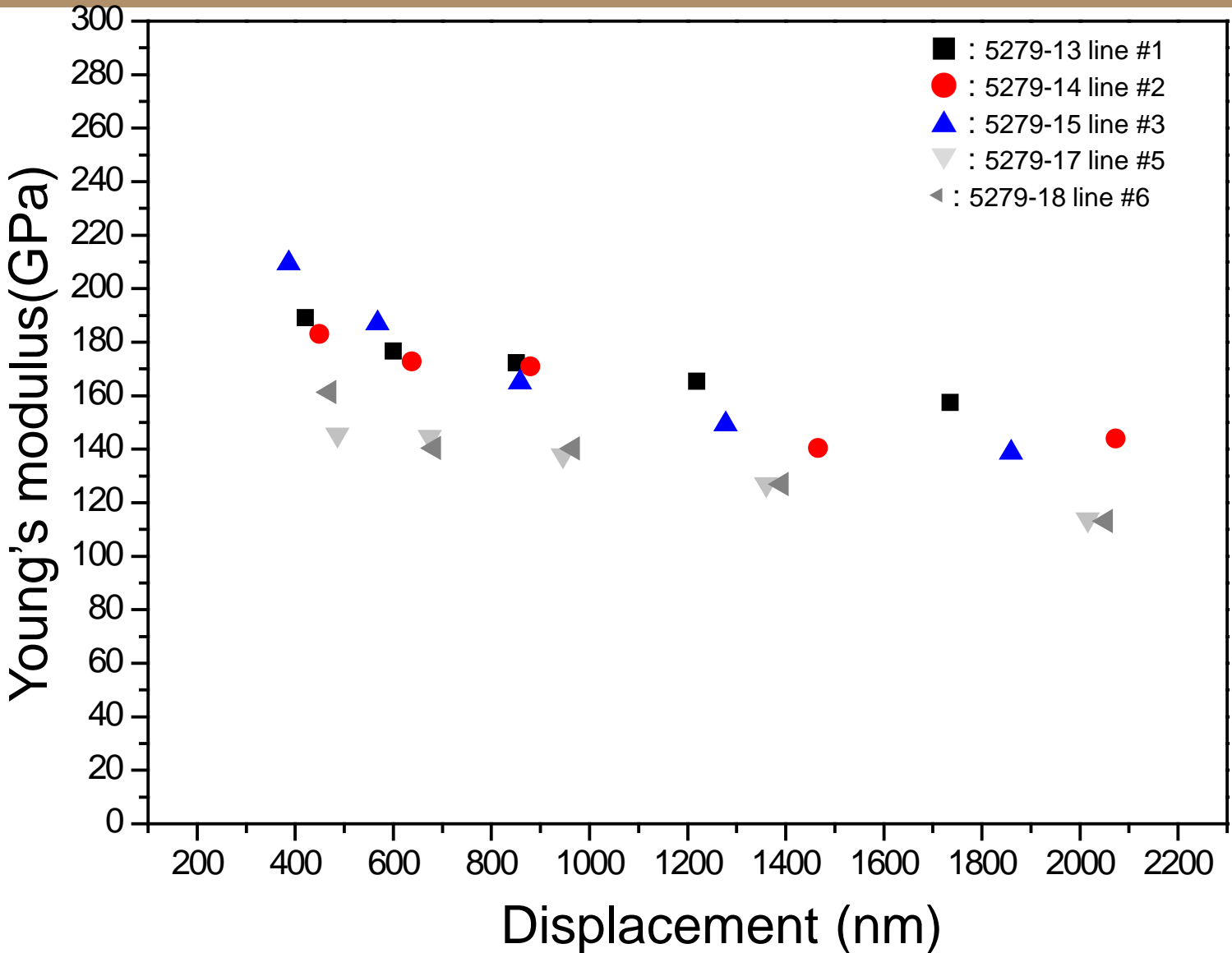


Bottom

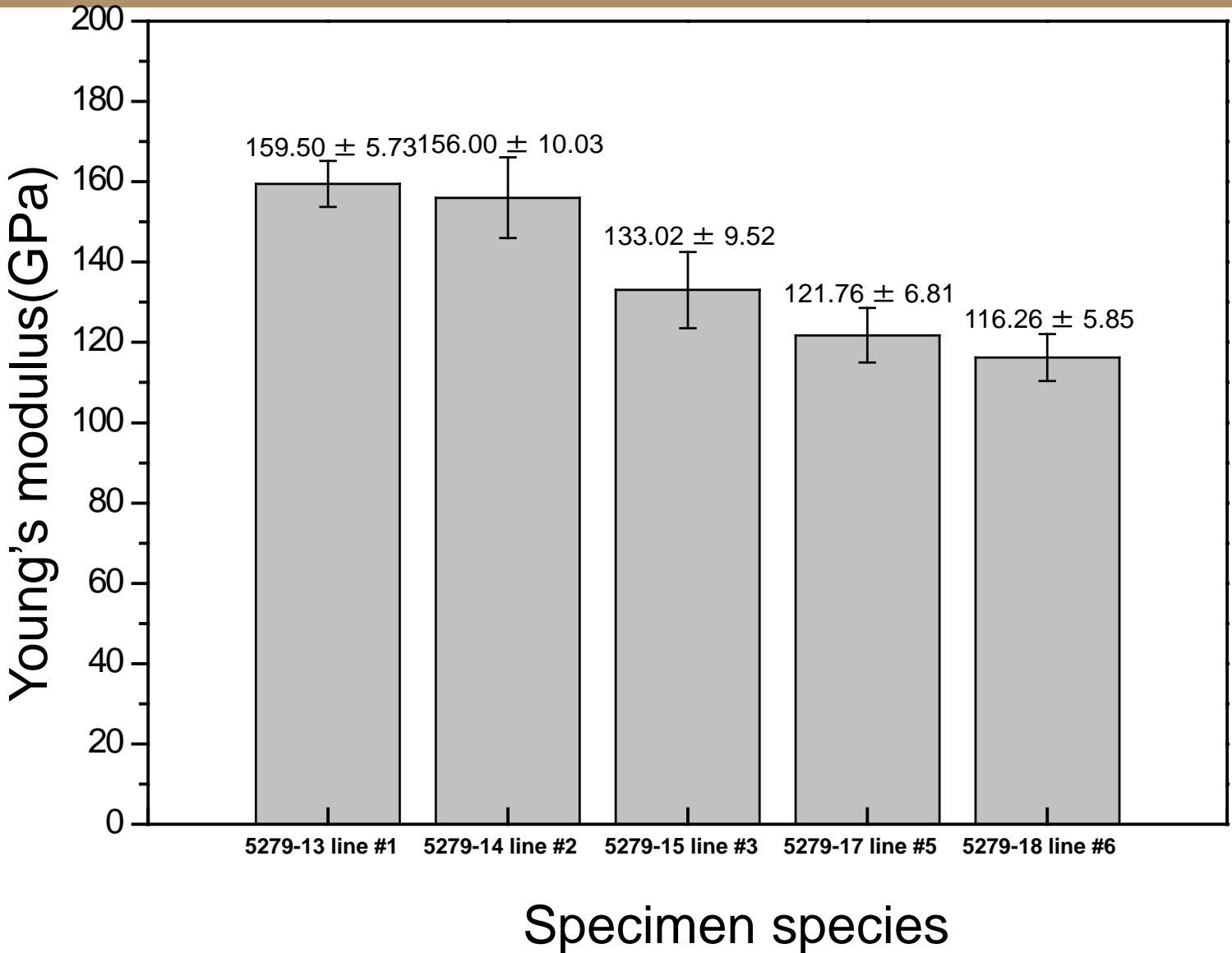
Nano-indentation



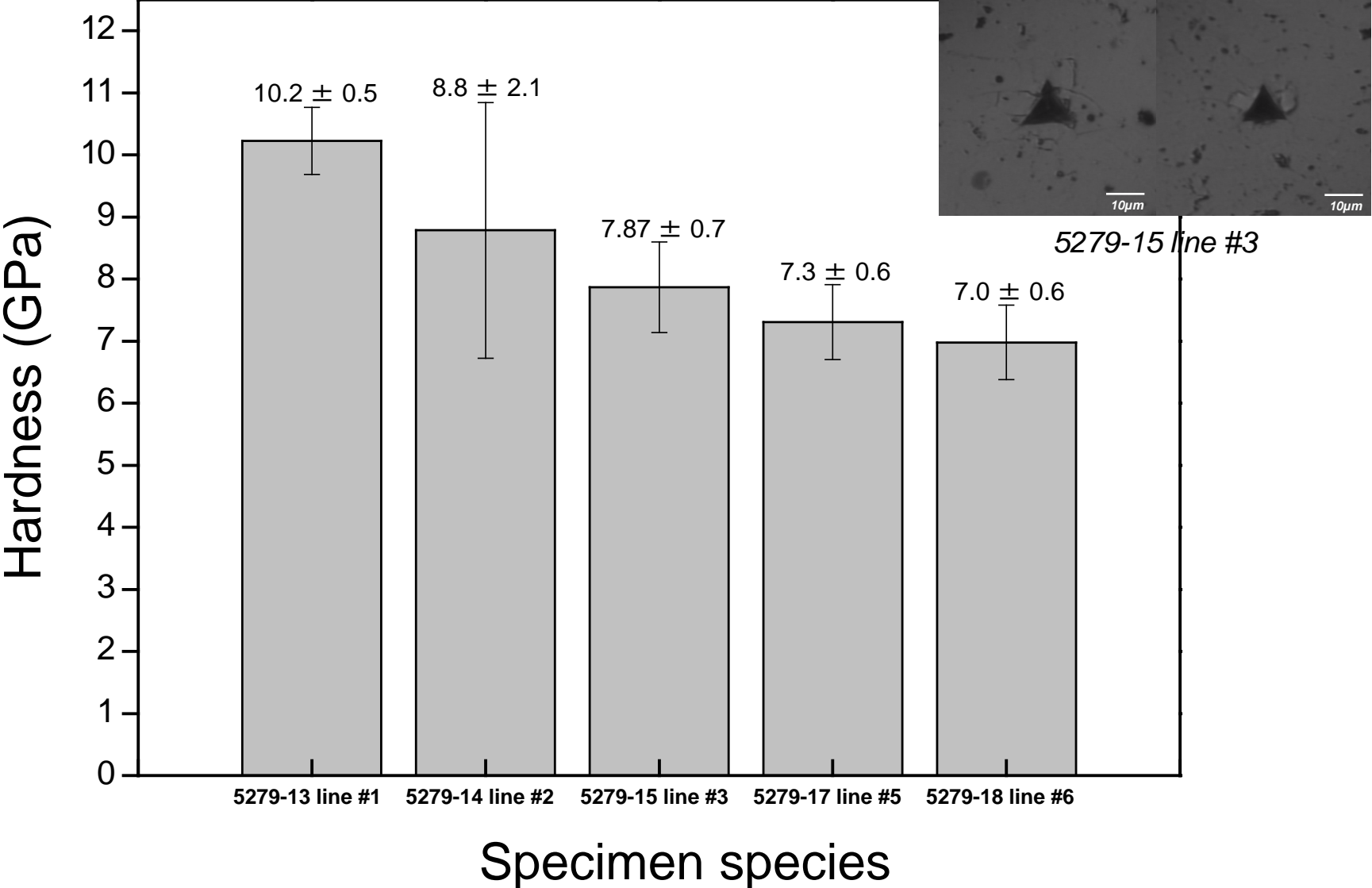
Summary of elastic moduli (from Nanoindentation)



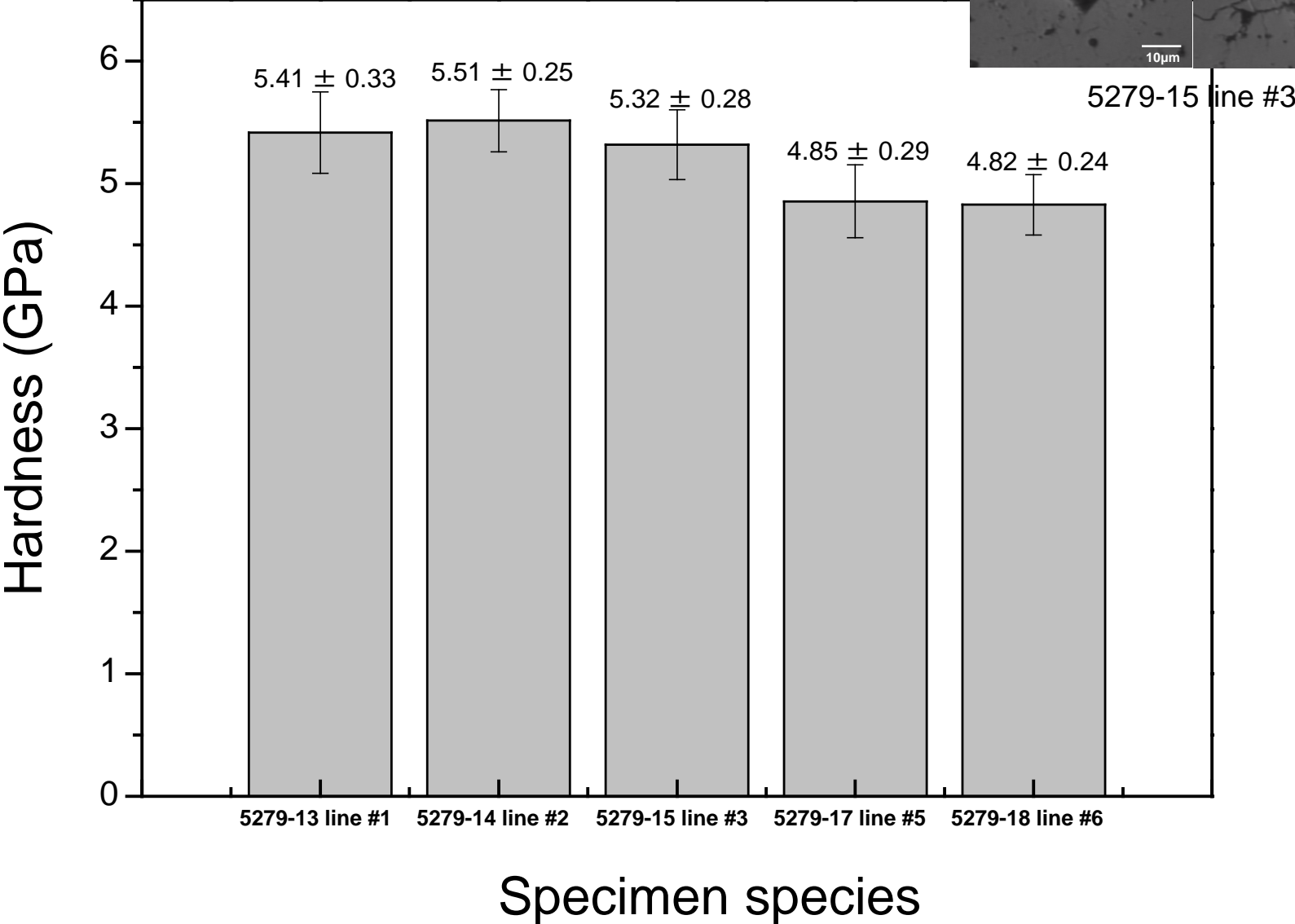
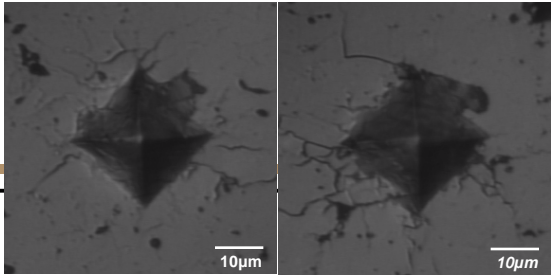
Summary of elastic modulus (from Nanoindentation)



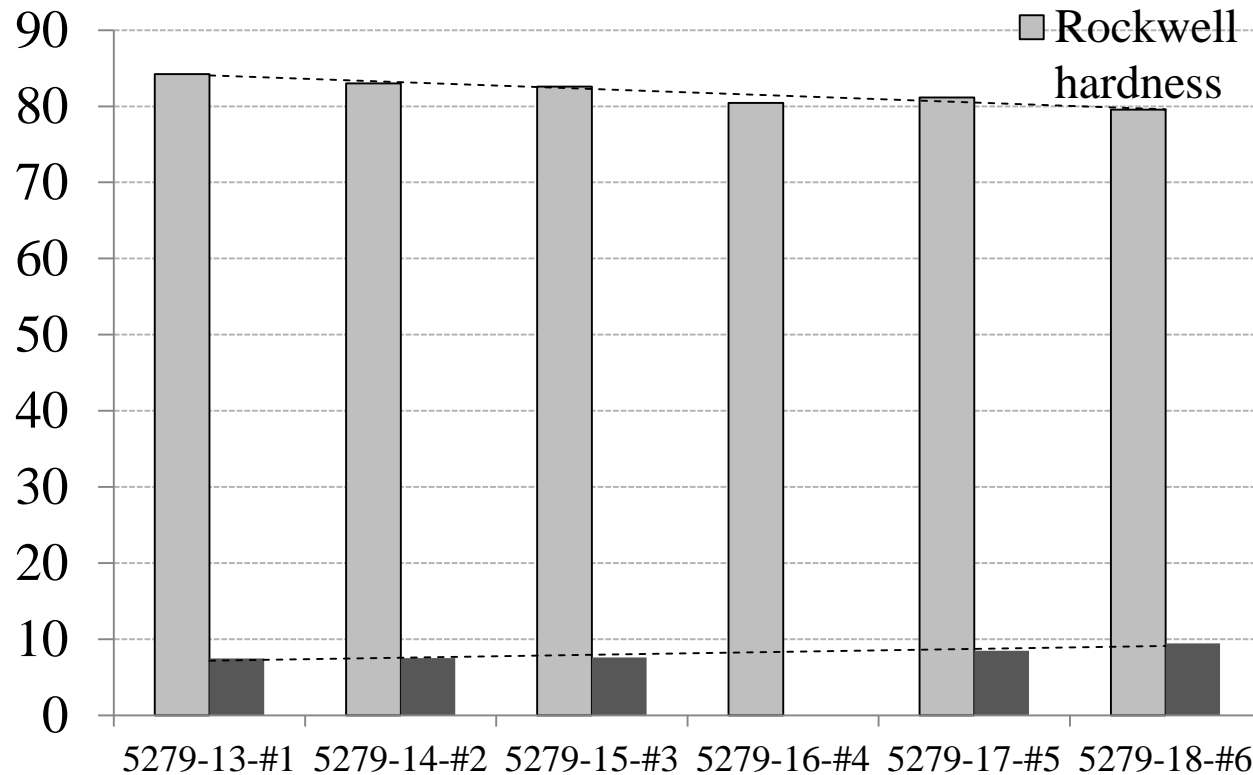
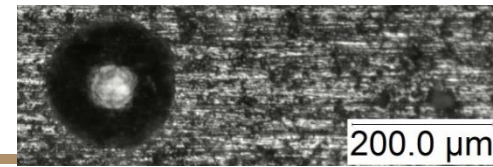
Summary of hardness (from Nanoindentation)



Summary of hardness (from Vicker's Indentation)



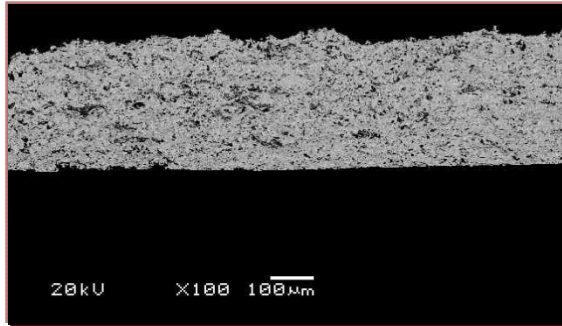
Summary of hardness (from Rockwell's Indentation)



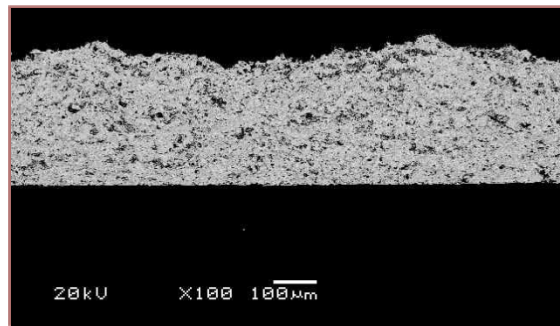
- Low density coatings with porosity between 7~10 % were achieved.
- Porosity and hardness can be tuned via changing processing conditions
- Powder feed rate \uparrow or current \downarrow \rightarrow porosity \uparrow \rightarrow hardness \downarrow
[Hardness = $1.99 \times (100 - \text{porosity}) - 100$]

- **I. Introduction**
 - $\text{La}_2\text{Zr}_2\text{O}_7$ vs. YSZ
 - Multilayer TBC structure
- **II. Experiments**
 - High density $\text{La}_2\text{Zr}_2\text{O}_7$
 - **Low density $\text{La}_2\text{Zr}_2\text{O}_7$**
- **III. Theoretical study of properties of $\text{La}_2\text{Zr}_2\text{O}_7$**
- **IV. Summary**

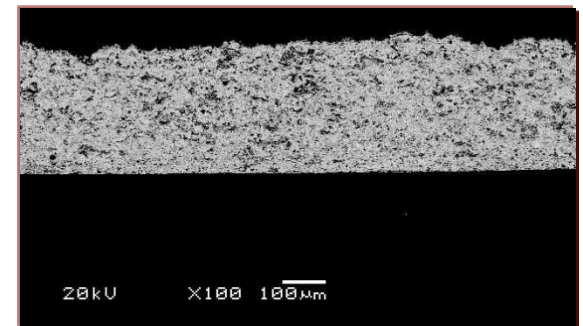
Low density coating



Position A



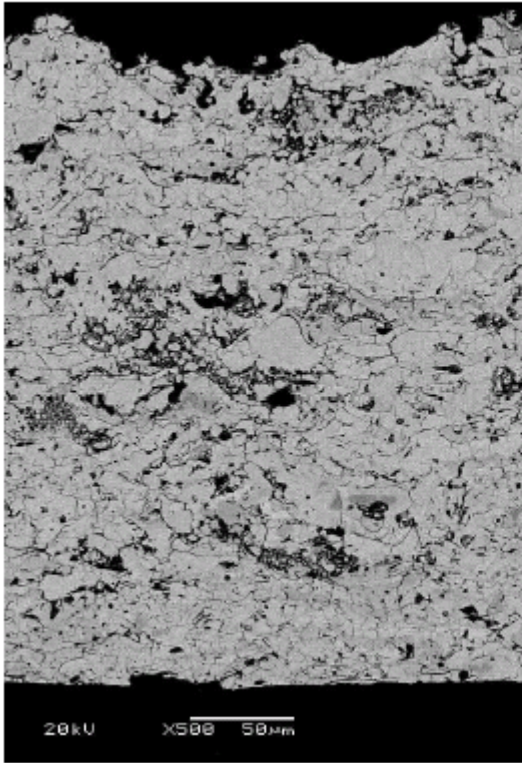
Position B



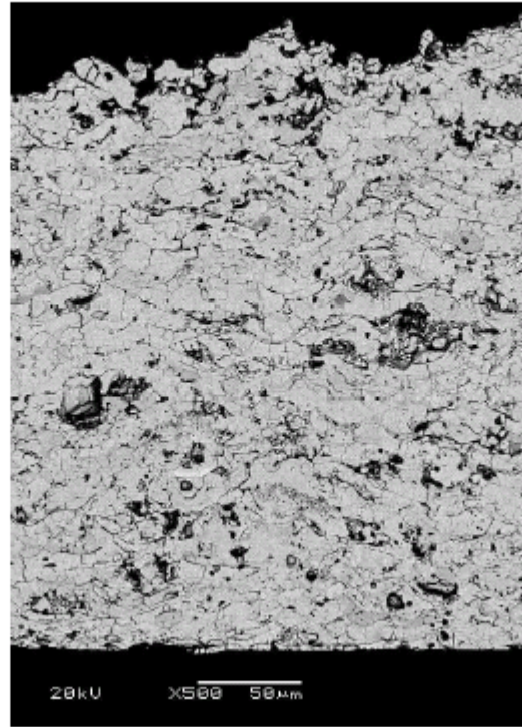
Position C

Line 12

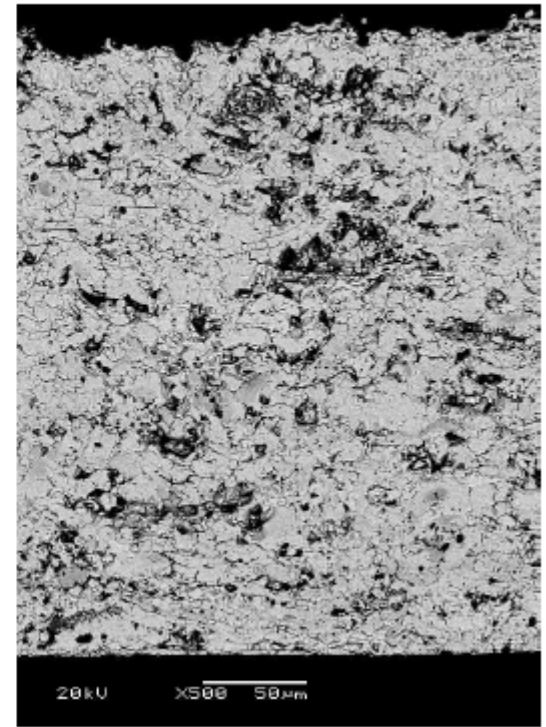
Low density coating (high mag.)



Position A

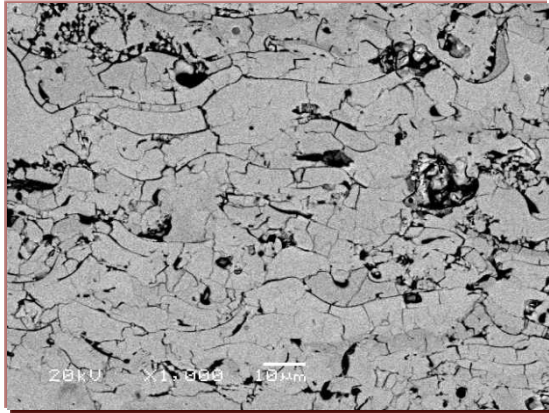


Position B

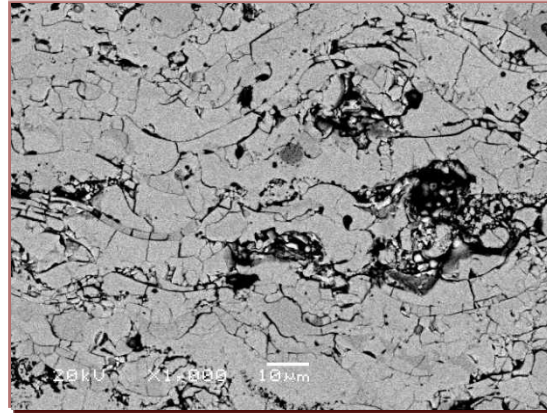


Position C

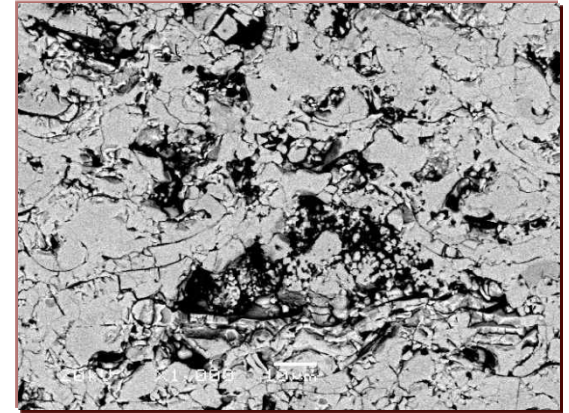
Low density coating (high mag.)



Position A

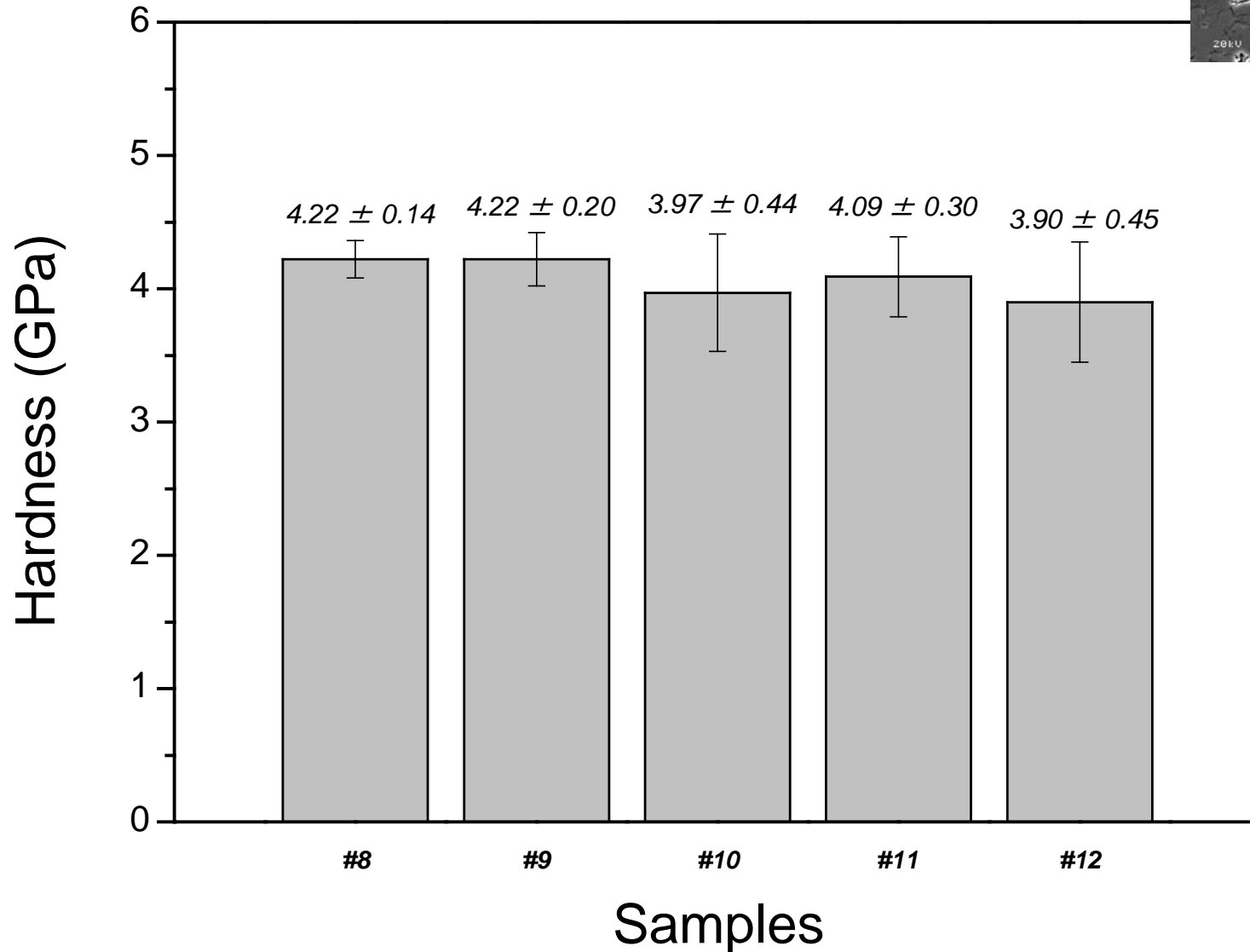
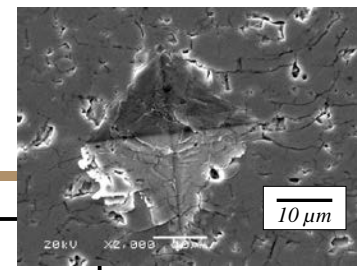


Position B

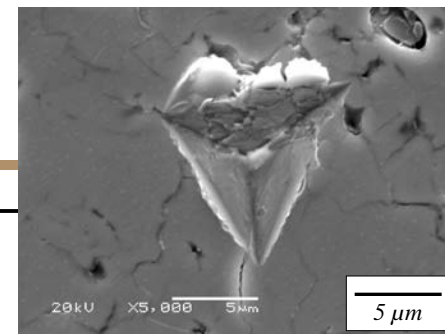
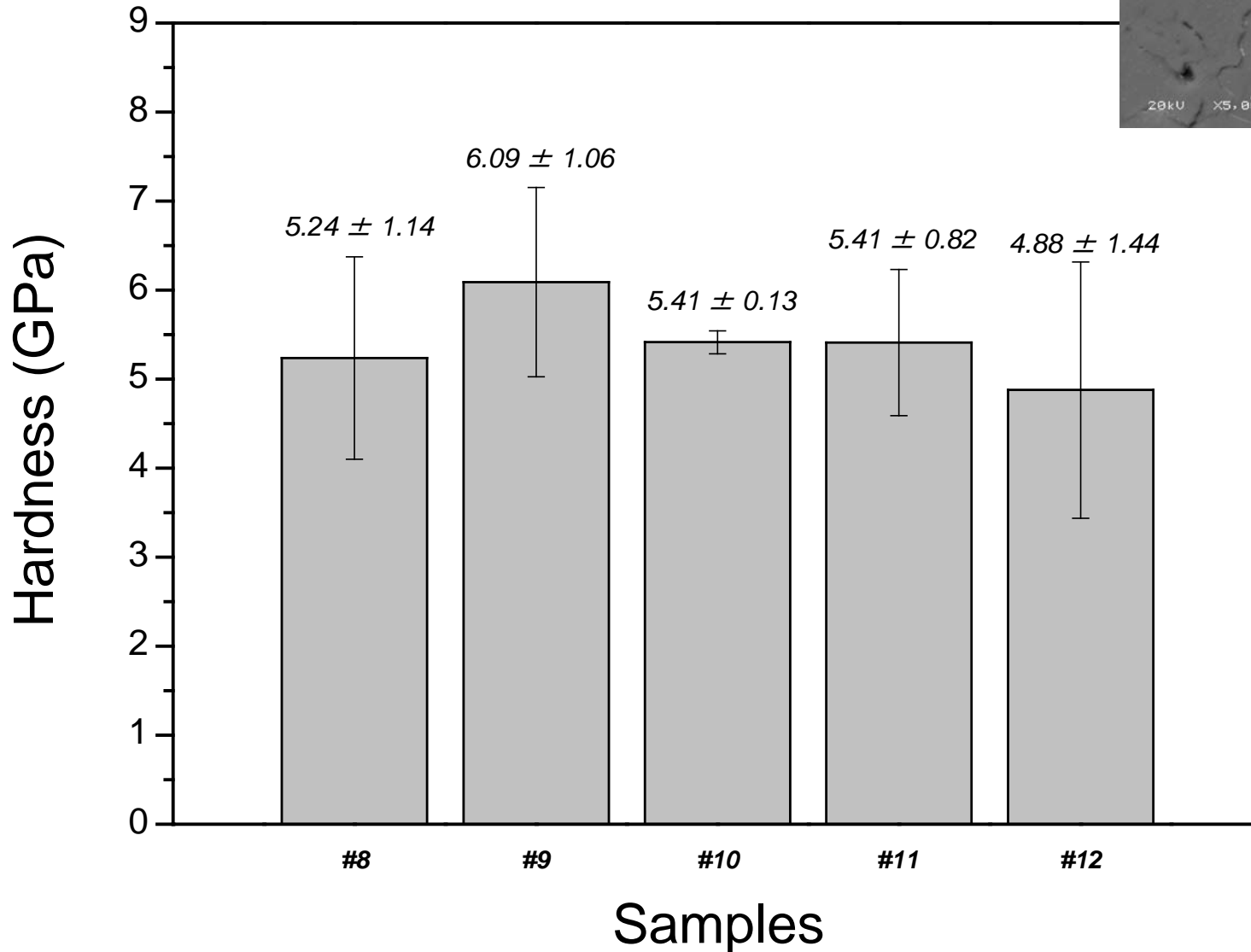


Position C

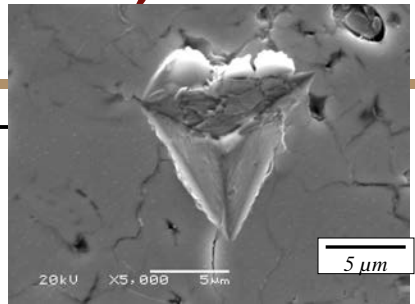
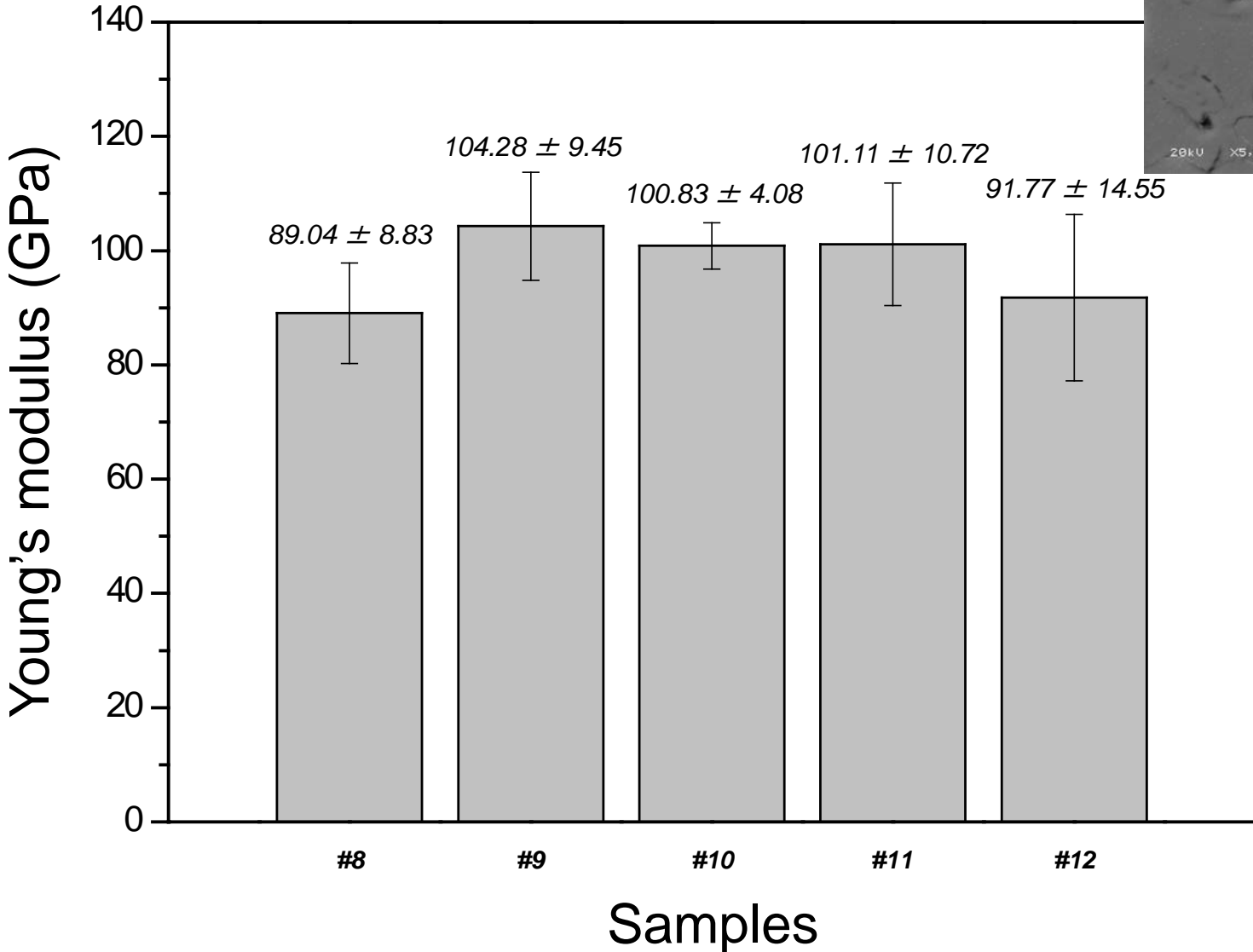
Summary of hardness (from Vickers indentation)



Summary of hardness (from nanoindentation)



Summary of Young's modulus (from nanoindentation)



Porosity of low density coating

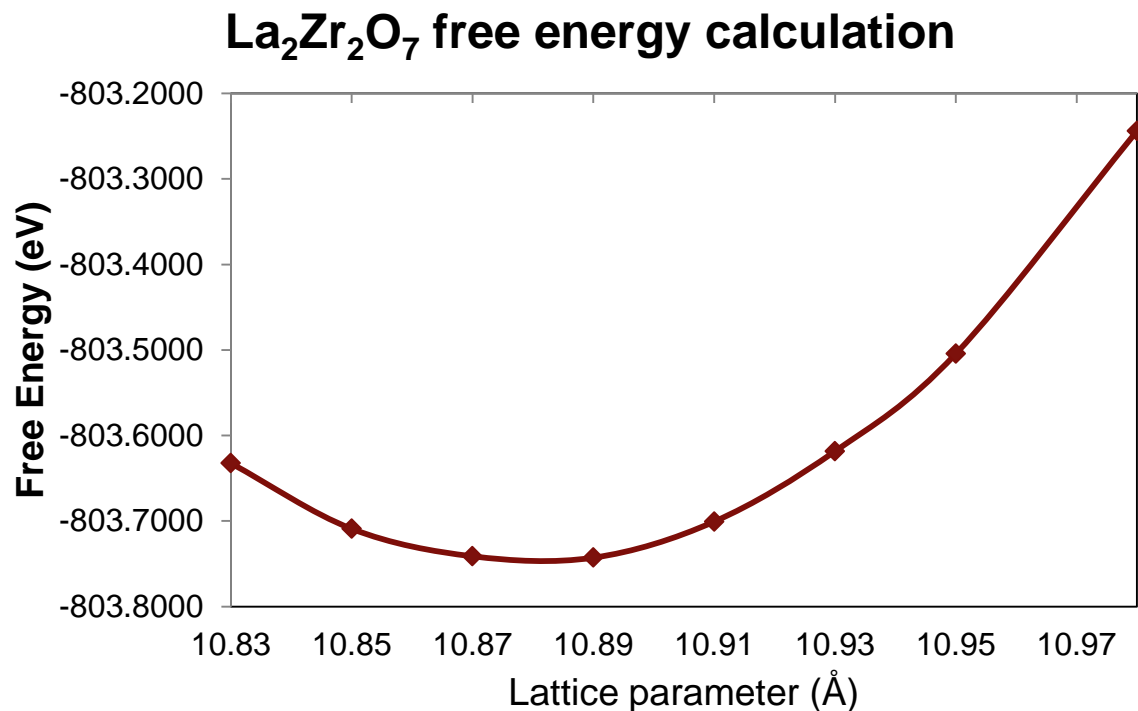
Line #	Batch #	Density (g/cm ³)	Porosity (%)	
Spray test	7	5279-19	5.3182	11.36
	8	5279-20	5.2587	12.36
	9	5279-21	5.2584	12.36
	10	5279-22	5.2917	11.81
	11	5279-23	5.2614	12.31
	12	5279-24	5.0089	16.52

Low density coatings with porosity between 11~17% were achieved.

Porosity = 1 - (Archimedes method density / fully dense density). Fully dense (theoretical) density is 6.0 g/cm³.

- **I. Introduction**
 - $\text{La}_2\text{Zr}_2\text{O}_7$ vs. YSZ
 - Multilayer TBC structure
- **II. Experiments**
 - High density $\text{La}_2\text{Zr}_2\text{O}_7$
 - Low density $\text{La}_2\text{Zr}_2\text{O}_7$
- **III. Theoretical study of properties of $\text{La}_2\text{Zr}_2\text{O}_7$**
- **IV. Summary**

Geometry optimization

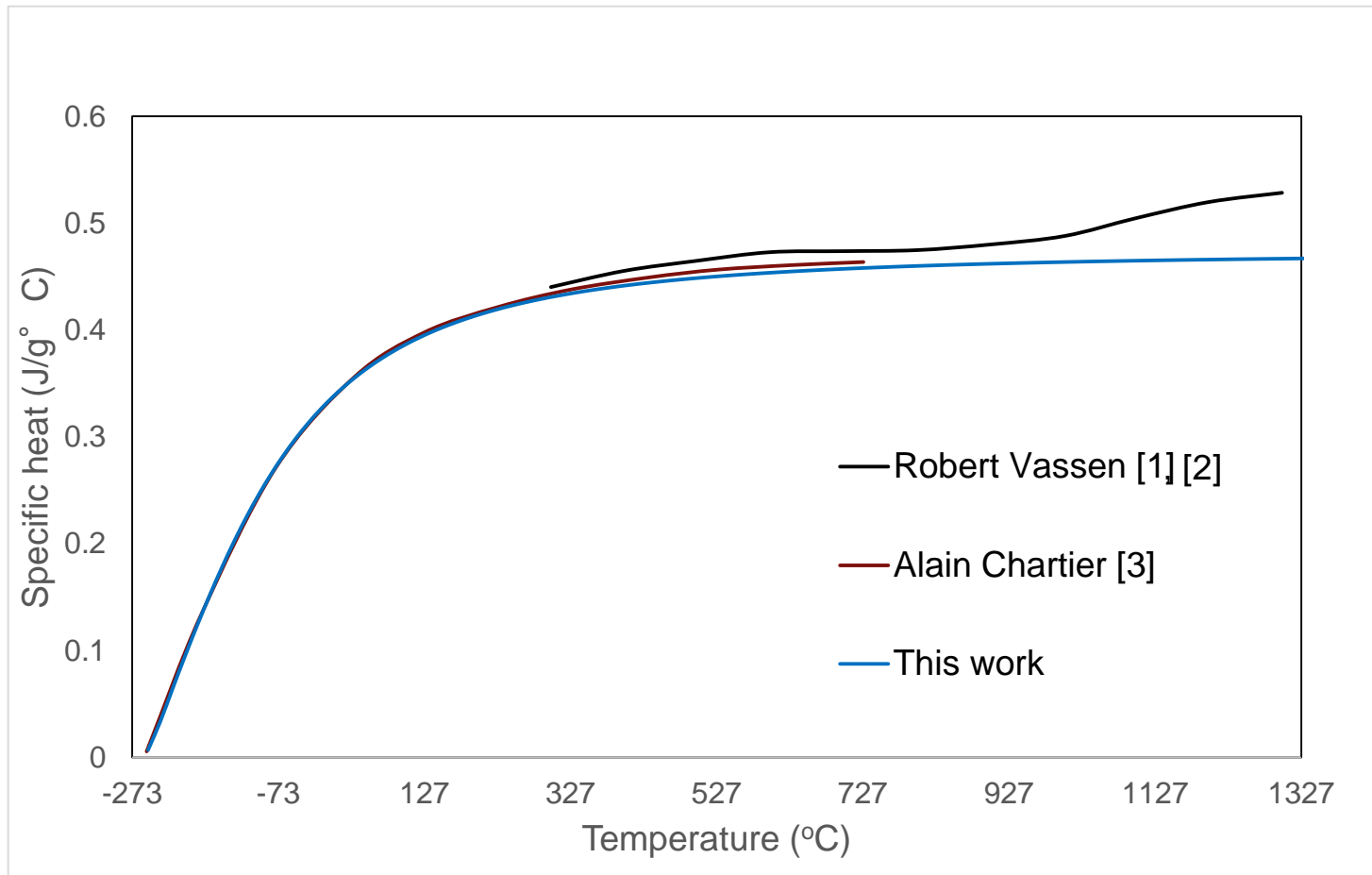


	Lattice parameter (Å)
This work (VASP)	10.89
This work (CASTEP)	10.73
Liu's work (CASTEP)	10.73
Tabira's work (XRD)	10.802

B. Liu et al, Acta Materialia, 55 (2007) 2949-2957.

Y. Tabira, et al, Journal of Solid State Chemistry, 153 (2000) 16-25.

La₂Zr₂O₇ specific heat (C_p) calculation



1.R. Vassen, et al, *J. Am. Ceram. Soc.* 83 (2000) 2023–2028.

2.H. Lehmann, et al, *Journal of the American Ceramic Society*, 86 (2003) 1338-1344.

3.A. Chartier, et al, *Physical Review B*, 67 (2003).

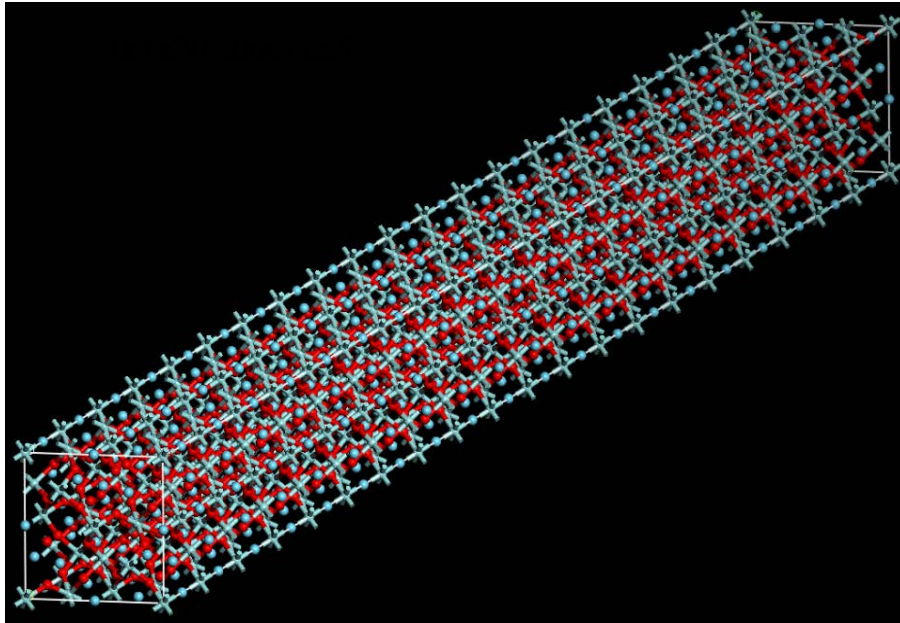
La₂Zr₂O₇ elastic constants calculation

- Both stress and strain have three tensile and three shear components, giving 6 components in total. The linear elastic constants form a 6 × 6 symmetric matrix, having 27 different components.
- For *Fm* $\bar{3}$ *d* cubic structure there are only 3 independent elastic constants C_{11} , C_{12} , C_{44} .

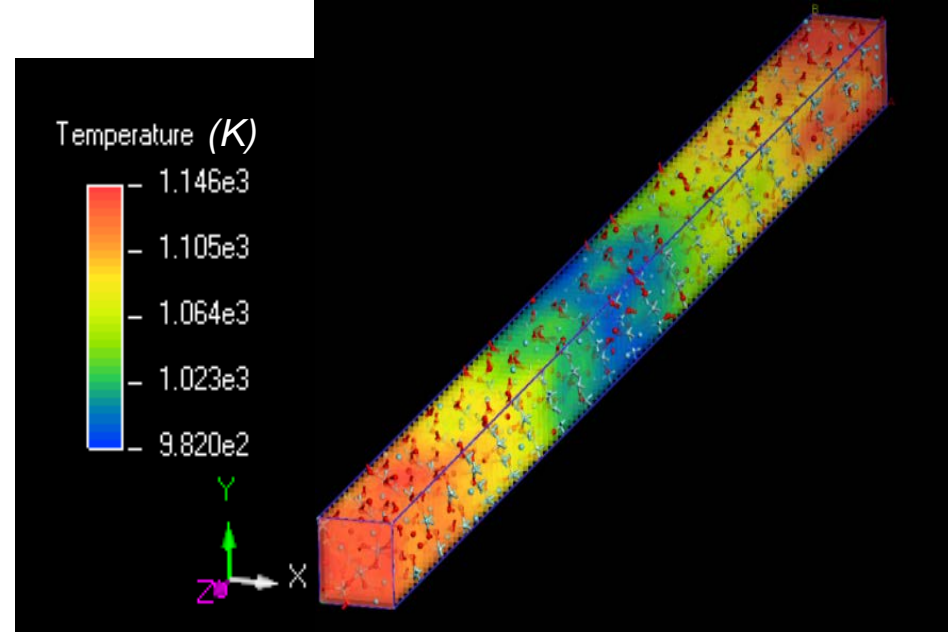
$$\begin{bmatrix} \varepsilon_x \\ \varepsilon_y \\ \varepsilon_z \\ \gamma_x \\ \gamma_y \\ \gamma_z \end{bmatrix} = \begin{bmatrix} C_{11} & C_{12} & C_{13} & C_{14} & C_{15} & C_{16} \\ C_{21} & C_{22} & C_{23} & C_{24} & C_{25} & C_{26} \\ C_{31} & C_{32} & C_{33} & C_{34} & C_{35} & C_{36} \\ C_{41} & C_{42} & C_{43} & C_{44} & C_{45} & C_{46} \\ C_{51} & C_{52} & C_{53} & C_{54} & C_{55} & C_{56} \\ C_{61} & C_{62} & C_{63} & C_{64} & C_{65} & C_{66} \end{bmatrix} \begin{bmatrix} \sigma_x \\ \sigma_y \\ \sigma_z \\ \tau_x \\ \tau_y \\ \tau_z \end{bmatrix}$$

	C_{11} (GPa)	C_{12} (GPa)	C_{44} (GPa)	Bulk modulus (GPa)	Shear modulus (GPa)
This work	289.8	124.8	100.4	179.8	93.3
Liu's work (CASTEP)	289	124	100	179	93

La₂Zr₂O₇ thermal conductivity calculation



Replicate 20 conventional cells along the heat flow direction to form a super cell



Calculated temperature contour based on Fourier's law $k = -\vec{q}''/\vec{\nabla}T$

The calculated thermal conductivity is 1.2 W/m/K at the temperature of 1000 °C, which is reasonably in agreement with the experimentally measured thermal conductivity ~1.5W/m/K [1].

[1] R. Vassen, X. Cao, F. Tietz, J. Am. Ceram. Soc., 83 (2000) 2023–2028.

Summary

- $\text{La}_2\text{Zr}_2\text{O}_7$ powder and coating's microstructure and chemistry characterizations show that $\text{La}_2\text{Zr}_2\text{O}_7$ is stable at high temperatures, which makes it suitable for TBC applications.
- Porosity of the coating can be controlled with desirable microstructures and mechanical properties.
- First principles studies of $\text{La}_2\text{Zr}_2\text{O}_7$ were conducted to derive fundamental thermal and mechanical properties.

Future work

- Fabricate multi-layer coatings using air plasma spray
- Characterize the coating using JETS and FCT tests
- Calibrate the model with experimental data

Publications

Materials Today - Proceedings

Co-editors: Jing Zhang, Yeon-Gil Jung, The 1st International Joint Mini-Symposium on Advanced Coatings between Indiana University-Purdue University Indianapolis and Changwon National University, Indianapolis, IN, USA, March 18~20, 2014

Xingye Guo, James Knapp, Li Li, Yeon-Gil Jung, and Jing Zhang, *ab initio* calculations of structural, thermal, and mechanical properties of lanthanum zirconate, 17th U.S. National Congress on Theoretical & Applied Mechanics, East Lansing, Michigan, 2014

Xingye Guo, James Knapp, Li Li, Yeon-Gil Jung, and Jing Zhang, *ab initio* study of the thermal and mechanical properties of lanthanum zirconate, Symposium Computational Design of Ceramic Materials, Materials Science & Technology 2014, Pittsburgh, Pennsylvania, 2014

Xingye Guo, James Knapp, Li Li, Yeon-Gil Jung, and Jing Zhang, Novel lanthanum zirconate based thermal barrier coatings for gas turbine applications, the 5th International Congress on Ceramics, Beijing, China, 2014